

# Regressor-Guided Generative Image Editing Balances User Emotions to Reduce Time Spent Online

CHRISTOPH GEBHARDT, Eastern Switzerland University of Applied Sciences & ETH Zürich, Switzerland

ROBIN WILLARDT, UNSW Sydney, Australia

SEYEDMORTEZA SADAT, ETH Zürich, Switzerland

CHIH-WEI "CHARLOTTE" NING, ETH Zürich, Switzerland

ANDREAS BROMBACH, ETH Zürich, Switzerland

JIE SONG, The Hong Kong University of Science and Technology (Guangzhou), China

OTMAR HILLIGES, ETH Zürich, Switzerland

CHRISTIAN HOLZ, ETH Zürich, Switzerland

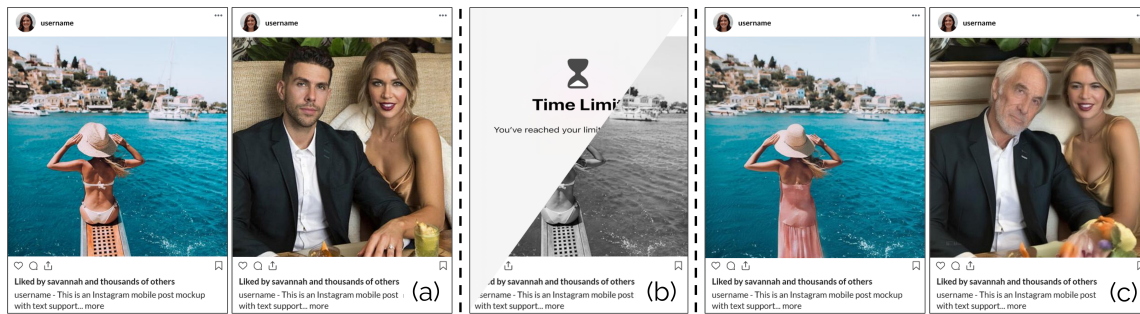


Fig. 1. Traditional approaches to reducing online engagement, such as time limits or image grayscale (b), can be restrictive and are often bypassed. We introduce three regressor-guided image-editing methods designed to lower images' emotional intensity without degrading visual quality. Our diffusion-based variant takes the original image (a) and, through classifier and classifier-free guidance, produces edited images that reduce emotionally salient cues (e.g., adding clothing, aging faces) (c). Our experiments show that presenting these edited images in a social media feed was associated with reduced usage duration and that they lowered perceived emotional intensity while maintaining high perceived quality.

Internet overuse is a widespread phenomenon in today's digital society. Existing interventions, such as time limits or grayscale, often rely on restrictive controls that provoke psychological reactance and are frequently circumvented. Building on prior work showing that emotional responses mediate the relationship between content consumption and online engagement, we investigate whether regulating the emotional impact of images can reduce online use in a non-coercive manner.

We introduce and systematically analyze three regressor-guided image-editing approaches: (i) global optimization of emotion-related image attributes, (ii) optimization in a style latent space, and (iii) a diffusion-based method using classifier and classifier-free guidance. While the first two approaches modify low-level visual features (e.g., contrast, color), the diffusion-based method enables higher-level changes (e.g., adjusting clothing, facial features).

Results from a controlled image-rating study and a social media experiment show that diffusion-based edits balance emotional responses and are associated with lower usage duration while preserving visual quality.

CCS Concepts: • **Human-centered computing** → **Human computer interaction (HCI)**; **Empirical studies in HCI**; • **Computing methodologies** → *Computer vision*.

## 1 INTRODUCTION

The Internet stands as one of the most significant inventions of the 20th century. Among other benefits, it democratizes access to information and facilitates unprecedented ease of communication. However, alongside these benefits, its use can also yield adverse effects for users. Research increasingly links it to forms of addiction, including social media [2, 5], online gaming [122], and pornography [75]. This pattern of behavior, termed problematic Internet use (PIU), involves difficulty controlling Internet activity. While prevalence estimates vary, recent data highlight the growing scale of the issue. For instance, PIU rates among adults are estimated at 10.1% in the United Kingdom and 10.4% in the United States [73], and are even higher among adolescents (e.g., 31% in Canada [67]). Users also report that the Internet distracts from work [46] and wellbeing [20], leading many to seek ways to reduce their usage [79].

To support users in managing their Internet consumption, a variety of tools have been introduced through research [61, 63, 77] and commercial products [6, 36, 42, 109]. However, these tools often impose strict restrictions (e.g., time limits) that provoke psychological reactance and are frequently circumvented [81]. Consequently, researchers argue that effective interventions should be sufficiently enforcing to change behavior without being perceived as overly coercive [79].

Meanwhile, marketing research highlights the pivotal role of emotions in shaping online behavior. Emotional experiences characterized by positive valence [38] and, to an even greater extent, heightened arousal levels [8, 92], boost online engagement. This suggests that emotional processes mediate the relationship between digital content consumption and online engagement [108, 123]. Similarly, Psychology has shown that image properties such as saturation, brightness, or subject beauty affect viewers' emotional responses [7, 68, 103]. Together, this indicates that changing the emotional properties of images may provide an indirect mechanism to influence online behavior.

Based on this evidence, we explore whether modifying the emotional impact of images can support non-coercive reductions in online use. We aim to regulate users' emotional states toward balanced valence and low arousal, encouraging natural disengagement rather than enforcing control. Therefore, we propose and systematically analyze three generative image-editing approaches. All approaches are guided by a regressor grounded in a psychological model of emotion [106], ensuring that edits move images toward the intended emotional state (neutral valence, low arousal). First, we optimize low-level image properties (e.g., brightness, contrast) that have been theoretically linked to emotional responses (e.g., [7, 103]). Second, we use a generative adversarial network (GAN) to disentangle content and style [54] and optimize style toward a subdued emotional response. Third, we employ a diffusion model (DM) [99] and leverage classifier guidance (CG) [34] and classifier-free guidance (CFG) [51] to steer the denoising process of an inverted image toward a visually similar but emotionally milder version.

Across the three approaches, our dual objective is to maintain visual quality and fidelity while enabling meaningful emotional modifications. Importantly, we intentionally vary the degree of change each method can introduce: while the first two techniques primarily adjust low-level visual attributes (e.g., contrast, color), the diffusion-based approach enables high-level visual changes such as altering clothing or facial expressions.

Our technical analysis shows that the proposed algorithms move images closer to the emotional reference than baseline approaches while maintaining high visual quality (according to KID and FID). Furthermore, the resulting emotional property changes are directionally consistent with prior research, with alignment observed for contrast, colorfulness, and blur.

In a controlled image-rating experiment ( $N = 48$ ), we find that only the diffusion-based variant produces changes in perceived emotions in the direction that is consistent with the emotional reference. It yielded valence ratings not

significantly different from neutral (t-test,  $p > .05$ ) and elicited significantly lower arousal than the original images (t-test,  $p < .05$ ); only grayscaling, which is already deployed in mobile operating systems as a digital well-being feature, achieved comparable reductions in arousal. However, unlike grayscaling, the diffusion-based method did not reduce perceived visual quality relative to the original images (t-test,  $p > .05$ ).

Motivated by these findings, we conducted a social media experiment ( $N = 188$ ) to examine whether diffusion-based edits influence browsing duration within a feed. Qualitative analysis indicated that the edited images introduced changes (e.g., reductions in perceived attractiveness or lower levels of nudity; see Figure 1) that align with theoretical accounts of how visual content shapes emotional responses [1, 93]. Using these edited images in posts was associated with reduced browsing duration compared to using the original images (t-test,  $p < .05$ ).

Collectively, our technical, perceptual, and behavioral analyses provide a systematic evaluation of emotional image-editing strategies and indicate that diffusion-based editing uniquely reduced emotional responses and social media usage duration without compromising perceived image quality.

In summary, our contributions are:

- We introduce three regressor-guided image-editing approaches that enable emotional modification of visual content at different levels of abstraction (from low-level color adjustments to high-level content edits) while maintaining perceptual quality and fidelity.
- We report findings from a controlled image-rating study ( $N = 48$ ) that systematically evaluates these approaches and shows that only the diffusion-based variant produces emotionally neutral responses without reducing perceived visual quality.
- We present results from a social media study ( $N = 188$ ) indicating that diffusion-based edited images lead to a measurable reduction in participants' time spent on a social media feed.

Taken together, these contributions provide empirical evidence and algorithmic design insights for emotion-aware image editing as a subtle, non-coercive strategy for supporting healthier patterns of online behavior.

## 2 RELATED WORK

Our work relates to the influence of emotions on online behavior, digital self-control tools, generative/computational methods for adapting images to modulate emotions, and the influence of image properties on emotional responses.

### 2.1 The role of emotions in online behavior

Research in marketing and psychology has explored how content influences emotions and, in turn, how these emotions affect online behavior. Emotions are commonly conceptualized using the Circumplex Model of Affect (CMA) [106], which characterizes them along two dimensions: valence, the degree of pleasantness, and arousal, the level of intensity.

Studies have shown that engaging with online discussions increases emotional arousal, with higher participation rates observed when users experience positive valence [38]. In the context of brand posts, it was found that high arousal or positive valence tend to boost user engagement [123].

On the other hand, research has found that emotions of negative valence, such as anger and disgust, are the driving factors behind the rapid spreading of false news [117]. Other work shows that high-arousal emotions like anger and disgust promote the spread of moral content, while low-arousal negative emotions such as sadness reduce spread [17].

It was also shown that high arousal content, regardless of its valence, drives virality [8]. Similarly, studies indicate that videos eliciting high arousal are more likely to be shared, while differences in valence have minimal impact [92]. A

meta-review of these and related findings concludes that there is evidence suggesting that high emotional arousal and positive valence tend to enhance engagement behavior [108].

In summary, these findings suggest that content which polarizes valence and elevates emotional arousal tends to increase online engagement levels. Based on these insights, our approach takes the opposite direction: it adjusts visual content to balance valence and decrease arousal, with the aim of reducing the time users spend online.

## 2.2 Digital self-control tools

Digital self-control tools (DSCTs) are applications that help users to follow their own long-term goals by avoiding digital distractions and unwanted habitual use. These tools mostly focus on increasing productivity or reclaiming free time [36, 42, 109]. Specialized DSCTs for parental control [100] or to avoid porn [25] are also available. Tools employ a wide range of strategies to increase self-control, e.g., hiding content on distracting websites [57], limiting functionality [88], gamification [35], or visualize time spent online [6].

Human-computer interaction (HCI) research (e.g., [64, 74, 80, 90, 98, 115]) has also investigated design patterns that help users regulate internet use, e.g., blocking distractions [61], reminding users about their long-term goals [63].

However, prior work and applications mostly rely on simple decision heuristics to constrain digital media use. This often results in overly severe restrictions (e.g., time limits) that trigger psychological reactance [18, 78] and, hence, are regularly circumvented [81]. This is why researchers advocate for the development of intervention mechanisms that are enforcing enough to change users' behavior without feeling too coercive [79]. In response, recent work leverages implicit input manipulation techniques to disrupt the execution of user gestures on mobile devices to reduce usage [77]. However, these techniques still depend on inducing frustration, and thus negative affect.

In contrast, our approach encourages natural disengagement by regulating emotional states toward balanced valence and low arousal, without enforcing breaks or inducing negative affect. At the same time, our image adaptations are designed to preserve visual quality and fidelity to the original content, creating interventions that are sufficiently impactful to provoke meaningful behavioral change while remaining subtle enough to preserve user autonomy.

## 2.3 Computational approaches to emotional image adaptation

Various approaches have been applied to adapt the emotional response that images elicit in viewers<sup>1</sup>. We organize prior work into three categories: approaches based on standard image transformations, methods that leverage generative adversarial networks (GANs), and more recent techniques employing diffusion models (DMs).

*2.3.1 Image transformations.* Several studies have explored the use of non-photorealistic rendering algorithms that produce stylized images to alter emotional responses. These works found that such algorithms tend to shift intense emotions toward a more neutral state, often due to the introduction of confusion or the loss of detail [91]. Additionally, these techniques have been shown to reduce the repulsiveness of images perceived as disgusting [13].

Early efforts in computer vision use neural networks to identify the distribution of emotions an image elicits and employ standard image transformations to change its affect towards a target emotional state [3, 96].

Another method selects a reference image based on emotional vocabulary and then optimizes the latent vectors in intermediate layers of a neural network to align an input image with this reference [4].

<sup>1</sup>In this review, we focus on techniques that adjust the emotional impact of arbitrary visual content rather than works that manipulate the expressions of depicted faces, which constitute a distinct research direction.

2.3.2 *GAN-based methods.* Various works in computer vision also used GANs to adapt the affect of images. For instance, GANs have been used to adapt source images so their emotional distributions align with a target domain, enabling cross-dataset emotion classification [124, 125]. Building on content and style disentanglement [54, 69], other GAN-based methods transfer the style of an emotional reference image to an input image. This can be done globally [126] or at the object level using semantic segmentation and multiple reference images for different objects [24].

While the approaches presented above used reference images to represent a target emotional state, other works rely on emotional classifiers or regressors to generate images based on specified sentiments. For instance, a specialized GAN architecture has been proposed to generate emotional landscape images from noise, guided by reference values in the valence-arousal space [94]. Another approach modifies the latent noise vector of a pre-trained GAN to shift images’ valence, using a regressor to verify if the desired emotional change was achieved [43].

2.3.3 *Diffusion-based methods.* Recently, DMs have surpassed GANs in terms of image synthesis quality [34, 50, 105]. As a result, research has explored how DMs can be used to modify the emotional properties of images. Several approaches fine-tune Instruct-Pix2Pix [19] on emotion-annotated data in order to adapt an input image to a target emotion while preserving scene structure, guided by a discrete emotion label (e.g., happiness, fear) [71, 121]. Building on this idea, a multi-agent framework extends these one-to-one emotion-visual mappings and can generate multiple visually distinct yet emotionally consistent edits from the same input image and target emotion [83].

More recent work moves beyond discrete categories and conditions diffusion models on textual prompts together with valence-arousal coordinates. One line of work integrates an emotion-embedding network to fuse valence-arousal values into textual features, aligning generated images with the emotional intent of the prompt [29]. Another approach applies reinforcement tuning to the DM, where a vision-language model evaluates the valence-arousal values of generated images and provides emotion-based rewards [58]. Similarly, another method optimizes an emotion token appended to the text embedding of a diffusion model, using a loss predicted by off-the-shelf emotion classifiers applied to the estimated clean image at each timestep, working for both generation from noise and image adaptation [119].

To enable a systematic evaluation across the three categories of prior work, we introduce representative approaches for each. First, we implement an *image-transformation-based* method and a *GAN-based* method that rely solely on an emotional regressor to adapt an input image, enabling theoretically grounded emotional image adaptation. Prior methods generally require example images that display the target emotion, which limits their applicability to arbitrary visual content in our setting. Despite being less expressive, we purposely include the *image-transformation-based* method as a computationally inexpensive baseline for low-level image attribute modification.

Second, existing *diffusion-based* methods typically rely on the attention mechanism of the U-Net to induce emotional changes, using either classifier-based losses or emotionally neutral prompt conditioning. However, prior research has shown that under high guidance weights such mechanisms can yield images with excessively salient colors, oversaturation, or overly glossy rendering [59, 107]. These effects are also visible in the qualitative results reported in the diffusion-based approaches mentioned above. Such artifacts are inconsistent with our goal of producing emotionally neutral, low-arousal images. For this reason, we design a *diffusion-based* approach that introduces emotional changes via gradients from an emotional regressor, thereby avoiding these artifacts.

## 2.4 The impact of image properties on emotional response

Psychology research shows that specific image properties shape viewers' emotional responses. To structure this review, we distinguish between low-level color and light properties, mid-level structural and spatial properties, and high-level content, each addressed in the subsections below.

*2.4.1 Low-level: Color and light properties.* Research shows that image attributes related to color and brightness strongly influence emotional responses. Increased *brightness* elicits more positive emotions, is consistently preferred across stimuli, and is recognized as a universal emotional factor across cultures [37, 113]. *Color* enhances emotional valence compared to grayscale as seen in brain responses [21] and make unpleasant scenes appear more negative and arousing [7]. Higher *saturation* is also linked to more positive ratings across affective image databases [103, 110]. Finally, increasing *contrast* raises valence, whereas reducing it lowers valence with only minor effects on arousal [120].

*2.4.2 Mid-level: Structural and spatial properties.* Structural and spatial features also shape emotional perception. Greater *variability in edge orientations* correlates with higher arousal [103], while *smooth contours* are rated more positively than angular ones [27]. Low-frequency color or grayscale changes evoke higher arousal regardless of valence [33], and reduced resolution or *blur* dampens both valence and arousal [31]. Finally, *symmetry*, widely considered a core aesthetic principle, is robustly associated with positive valence and arousal [10–12, 15, 82].

*2.4.3 High-level: Content.* Image content has a strong impact on emotional responses. For example, *nudity* has been shown to increase arousal [93], while viewing *attractive faces* consistently elicits positive emotions [1, 41, 48, 116]. Additionally, *complexity* is strongly linked to heightened arousal, as more complex images offer a variety of informational cues that capture attention and stimulate greater mental energy [9]. Moreover, the *personal semantic meaning* of an image has been found to have the most significant impact on emotional responses [55, 97].

Building on these prior studies, we select emotionally relevant image properties as optimization variables for our *image-transformation-based* method. We further employ these properties as evaluation metrics to determine whether the adapted images change in the theoretically consistent direction.

## 3 DESIGN CRITERIA FOR EMOTION-REGULATING IMAGE EDITING

Building on the insights from prior work, our goal is to support users in reducing their time spent online by regulating the emotional impact of online images without introducing visually unpleasant or overly pronounced changes. To operationalize this goal, we define four design criteria (referred to as *criteria* throughout the paper). Approaches should:

- (i) Balance emotional valence,
- (ii) Reduce arousal,
- (iii) Preserve overall image quality, and
- (iv) Maintain alignment with the original content.

By adhering to these criteria, the methods aim to enable behavioral change through natural disengagement rather than coercion, thereby minimizing the risk of psychological reactance and maintaining user autonomy.

To theoretically ground the adaptations in the Circumplex Model of Affect and to explicitly target a neutral valence and low arousal state, we employ a regression model that predicts valence and arousal in accordance with the CAM. This regressor provides the guiding signal for adaptation, enabling optimization toward the specified emotional reference.

## 4 METHOD

We propose three methods to adapt images according to the outlined design criteria. These methods systematically vary in the degree of modification they allow and in the computational resources they require. All approaches rely on the signal of a regressor that predicts the emotions an image is likely to elicit. In the following, we first describe the training of the regressor and then detail the implementation of each approach.

### 4.1 Emotion regressor

We train the emotion regressor by fine-tuning a pre-trained ResNet50 model (ImageNetV2) on a custom dataset composed of multiple emotional databases. Specifically, we integrate NAPS [82], DIRTI [47], CGnA10766 [60], EmoMadrid [22], Emotion6 [96], GAPED [28], OASIS [65], OLAF [87], MAPS [44], and IAPS [66], which are open-science emotional image databases providing human valence and arousal ratings consistent with the CMA, resulting in a combined dataset of 20,460 images.

We apply min-max normalization to valence and arousal ratings across databases, mapping them onto a unified scale from 0 to 1. In the appendix, we provide a figure illustrating the positions of these images within the valence-arousal space of the CMA (see Appendix B). Our regressor achieves a mean absolute error of 0.11 for valence and 0.12 for arousal on a validation split.

In alignment with the defined *criteria* as well as the CMA and the value range after normalization, we set the *emotional reference* for the adaptation approaches to a valence value of  $v' = 0.5$  and an arousal value of  $a' = 0.0$ .

### 4.2 Style optimization

Our style-optimization approach modifies a latent style code to alter only low-level image features while preserving the depicted content. To achieve this, we employ the MUNIT generator as a backbone to disentangle content and style [54] and optimize the latent style vector in alignment with our *criteria*. The overall approach is illustrated in Figure 2.

To optimize the latent style, we apply the emotion regressor to the adapted image and compute a loss based on the difference between the predicted emotional values and the *emotional reference* (*criteria i & ii*). In addition, we retain fidelity to the original image by incorporating the content-consistency loss proposed in MUNIT (*criterion iv*). Using the pre-trained MUNIT decoder helps preserve high image quality (*criterion iii*).

**4.2.1 Disentangling content and style.** MUNIT uses an autoencoder-based generator within a GAN framework to factorize an image into a content vector and a style vector for unsupervised style transfer across domains. We adapt this approach by training MUNIT’s GAN on ImageNetV2 to obtain a general-purpose content-style disentanglement, following a methodology similar to [126].

The model was trained for approximately 200,000 iterations, after which qualitative inspection and an FID of 3.2 on swapped-style images indicated effective disentanglement. Consistent with prior work [126], the generator learned to separate high-level content (e.g., objects, people) from low-level stylistic characteristics (e.g., color, texture, brightness).

**4.2.2 Optimization.** Given an input image, we use the trained generator to obtain its content and style codes. The style code serves as the initialization for optimization, which we formulate as

$$\arg \min_{s \in \mathcal{S}} w_1 |E_c(I) - E_c(D(E_c(I), s))| + w_2 \|[v', a'] - R(D(E_c(I), s))\|. \quad (1)$$

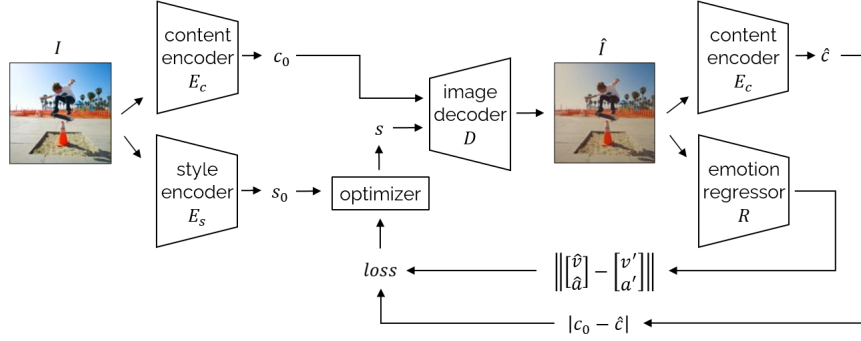


Fig. 2. Style optimization: To adapt an input image  $I$ , its latent style vector  $s$  is optimized to generate a similar image that elicits a reduced emotional response when decoded with  $I$ 's latent content  $c_0 = E_c(I)$ , resulting in  $\hat{I} = D(c_0, s)$ . The optimization process minimizes the distance between the predicted valence and arousal of the adapted image,  $[\hat{v}, \hat{a}] = R(\hat{I})$ , and the target values specified by *emotional reference*,  $[v', a']$ . Additionally, the optimization incorporates a term to ensure content consistency by minimizing the L1 loss between the encoded latent content of the generated image,  $\hat{c} = E_c(\hat{I})$ , and  $c_0$ . The style vector  $s$  is initialized as the encoded style vector of the input image,  $s_0 = E_s(I)$ .

Here,  $R$  denotes the emotion regressor,  $[v', a']$  specifies the *emotional reference*,  $I$  is the input image, and  $E_c$  and  $D$  are the content encoder and decoder of MUNIT, respectively. The optimized style  $s$ , within the set  $\mathcal{S}$ , is initialized as  $s_0 = E_s(I)$ , where  $E_s$  is MUNIT's style encoder.

### 4.3 Parametric Optimization

This approach optimizes parameters of differentiable image transformations to modulate the emotional response an image elicits. A key advantage is that the inferred parameters can be applied to images of arbitrary resolution and transferred to sequential frames of a video, as demonstrated in prior work [86]. By relying on global transformations, the method intentionally targets only low-level image properties, ensuring that the depicted content remains unchanged.

To ground the method theoretically, we adapt image properties that have been shown to influence emotional responses (see Sec. 2.4). Specifically, we apply global transformations that adjust *brightness* (exposure), *saturation* (tone curves [86]), *color* (color curves [53]), *contrast*, *sharpness* (via sharpening and blurring), *overall blur*, and *symmetry* (via translation and scaling).

The objective function leverages the emotion regressor to guide the adaptation towards the *emotional reference* (criteria *i* & *ii*). In addition, we impose a loss on the CLIP embeddings [101] of the input and output images to preserve semantic similarity, which also indirectly constrains visual quality (criteria *iii* & *iv*). Figure 3 illustrates the approach.

Specifically, the objective function of the parametric optimization is defined as:

$$\arg \min_{p \in \mathcal{P}} w_1 \mathcal{L}_{\text{CLIP}}(I, T(I, p)) + w_2 \left\| [v', a'] - R(T(I, p)) \right\| \quad (2)$$

where  $p$  represents the optimized parameters within the feasible set  $\mathcal{P}$ ,  $I$  is the input image,  $T$  is the differentiable image transformation function,  $R$  is the emotion regressor, and  $[v', a']$  defines the *emotional reference*. The term  $\mathcal{L}_{\text{CLIP}}(I, T(I, p)) = \frac{c \cdot \hat{c}}{\|c\| \|\hat{c}\|}$  defines the cosine similarity between the CLIP embeddings of the original image  $c = \text{CLIP}(I)$  and the transformed image  $\hat{c} = \text{CLIP}(T(I, p))$ .

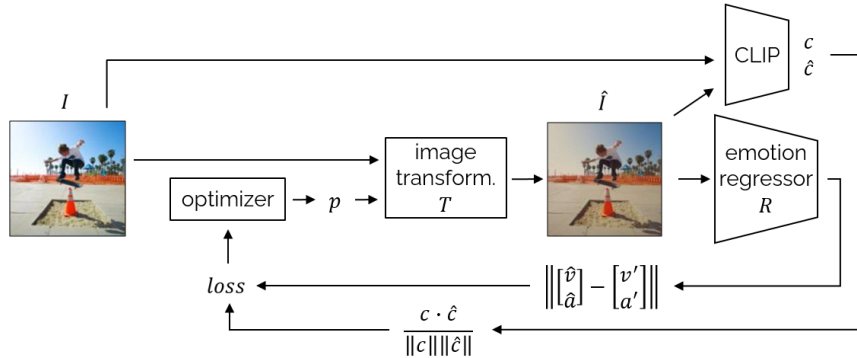


Fig. 3. Parametric optimization: To adapt an input image  $I$ , the parameters  $p$  of the differentiable image transformations  $T$  are optimized to produce a similar image that elicits a reduced emotional response, represented by  $\hat{I} = T(I, p)$ . The optimization minimizes the distance between the predicted valence and arousal of the adapted image,  $[\hat{v}, \hat{a}] = R(\hat{I})$ , and the *emotional reference*,  $[v', a']$ . It further ensures a high cosine similarity between the CLIP-space embeddings of the input image  $c = CLIP(I)$  and the transformed image  $\hat{c} = CLIP(\hat{I})$ .

#### 4.4 Regressor-Guided Diffusion Resampling (RGDR)

The third approach leverages a diffusion model to enable higher-level image adaptations while preserving overall image fidelity. Given an input image, RGDR first inverts it into its corresponding noise vector using the diffusion model’s noise prediction and an inverse deterministic scheduler [34, 111]. It then applies null-text optimization [89] to enhance editability of the latent representation. Subsequently, denoising is guided through two conditioning mechanisms: (1) classifier guidance (CG) [34], which steers the process toward neutral valence and low arousal (*criteria i & ii*); and (2) classifier-free guidance (CFG) [51], which incorporates the caption of the original image to preserve content alignment (*criterion iv*). Using a pre-trained diffusion backbone helps maintain high perceived image quality (*criterion iii*). Figure 4 provides an overview.

In the following, we formally detail each step of the proposed approach. For a background on diffusion models and the related methods that support our approach, please refer to Appendix A.

**4.4.1 Training the guidance regressor.** To enable CG, we train a regressor  $R_u$  that predicts valence and arousal values on the output of the middle layer of a diffusion model  $u_t$ :  $[\hat{v}, \hat{a}] = R_u(u_t)$ . This approach has two advantages over directly using the current noisy latent vector  $z_t$  as input. First, it is more memory-efficient, as it only requires tracing gradients through half of the diffusion model rather than the entire model during inference guidance. Second,  $u_t$  is a denser representation of  $z_t$ , filtering out irrelevant information and incorporating context about the current timestep  $t$ .

To train  $R_u$ , we first encode the images from our custom dataset (Sec. 4.1) into latent representations using the encoder of SDXL,  $z_0 = E(I)$ . We then add noise to these latents according to the forward diffusion process by randomly sampling a timestep  $t$ , resulting in  $z_t = \text{ForwardDiffusion}(z_0, t, \beta)$  (see App. A.1 for a definition of  $\beta$ ). These noisy latents, along with their corresponding timestep and the null-text embedding  $\emptyset$ , are passed through the diffusion model to obtain its middle-layer output  $u_t = DM_{\text{half}}(z_t, t, \emptyset)$ . The output  $u_t$  is then used as input to  $R_u$ , with valence and arousal ratings from the dataset serving as prediction targets. This process is repeated until performance stabilizes.

**4.4.2 Inverting the input image.** To adapt an image  $I$ , we first obtain its latent image encoding  $z_0 = E(I)$  and the text embedding of its caption  $C = \psi(\mathcal{P})$ . We then perform inverse DDIM to attain an optimized noise vector

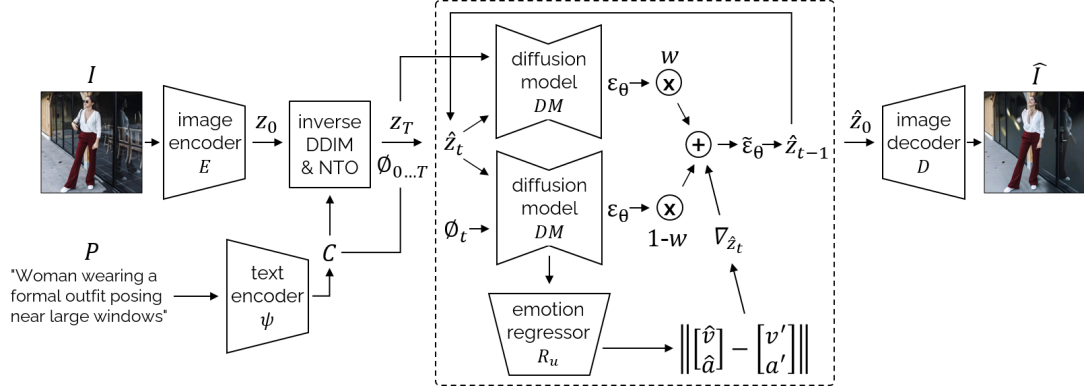


Fig. 4. Regressor-guided diffusion resampling: To adapt an input image  $I$ , it is first encoded into a latent vector  $z_0 = E(I)$  and then inverted to its corresponding noise vector  $z_T = DDIM_{\text{inv}}(z_0, t, C, \beta)$ , while generating unconditional text embeddings for each timestep  $\{\theta_t\}_{t=1}^T = NTO([z_T, \dots, z_0], C)$ , ensuring editability of  $\hat{z}_t$  and alignment with  $I$ . At each step of the denoising process,  $\hat{z}_t$  is updated by blending the predicted unconditional and conditional noise  $\epsilon_\theta$ , further refined by a score  $\nabla_{z_t}$  that quantifies alignment with the *emotional reference*. With the resulting noise vector  $\tilde{\epsilon}_\theta$ ,  $\hat{z}_{t-1}$  can be obtained. The final latent vector  $\hat{z}_0$  is decoded into the image  $\hat{I} = D(\hat{z}_0)$ , which closely resembles  $I$  while modulating the emotional response.

$z_T = DDIM_{\text{inv}}(z_0, t, C, \beta)$ . Next, we apply NTO to derive unconditional embeddings for each timestep  $\{\theta_t\}_{t=1}^T = NTO([z_T, \dots, z_0], C)$ . This ensures that during inference  $z_t$  remains editable and that the resulting image stays closely aligned with the input image [89].

**4.4.3 Dual-conditioned resampling.** In this step, we resample  $\hat{z}_0$  from  $z_T$  by conditioning the denoising process on the valence-arousal reference values  $v', a'$  and the caption embeddings  $C$ . During each timestep  $t$ , we condition the denoising trajectory by approximating the classifier guidance term using a score, computed as follows:

$$\nabla_{z_t} \log p_\phi(v', a' | \hat{z}_t) = \left\| [v', a'] - R_u(DM_{\text{half}}(\hat{z}_t, t, \theta)) \right\|^2, \quad (3)$$

where  $[v', a']$  defines the *emotional reference*. The noise prediction is then carried out with the modified objective:

$$\hat{\epsilon}_\theta(\hat{z}_t, t, C, \theta_t) = w \cdot \epsilon_\theta(\hat{z}_t, t, C) + (1 - w) \cdot \epsilon_\theta(\hat{z}_t, t, \theta_t) + s \cdot \nabla_{z_t} \log p_\phi(v', a' | \hat{z}_t). \quad (4)$$

Finally, we perform the standard DDIM update step to obtain  $\hat{z}_{t-1} = DDIM(\hat{z}_t, t, C, \beta)$ .

In summary, from a probabilistic perspective, our approach can be interpreted as a diffusion probabilistic model  $p_\theta(\hat{z}_0 | z_T, \mathcal{P}, v', a')$  that generates an adapted image latent  $\hat{z}_0$  conditioned on the noised latent vector of an input image  $z_T$ , its image caption  $\mathcal{P}$ , and specified reference values for valence  $v'$  and arousal  $a'$ .

## 5 IMPLEMENTATION

All approaches were implemented using PyTorch and operated on images at a resolution of  $1024 \times 1024$ .

For RGDR, we leveraged the stable diffusion model SDXL as its backbone [99]. Specifically, we used the Diffusers implementation of SDXL from Stability AI<sup>2</sup>. Since SDXL relies on a float16 tensor representation, using default null-text optimization led to vanishing gradients. To address this, we re-implemented NTO with mixed-precision capabilities.

<sup>2</sup><https://huggingface.co/stabilityai/stable-diffusion-xl-base-1.0>

The network of RGDR’s guidance regressor consisted of four convolutional layers, each followed by ReLU activation and max-pooling, before passing through two fully connected layers to produce the final output predictions.

To attain captions for images, we leveraged the GPT4 Vision 2024-05-01-Preview model of Azure OpenAI and prompted it to provide descriptive captions that could be used as labels for a machine learning dataset.

Both, parametric and style optimization, employed the Adam optimizer with parameters  $\beta_1 = 0.9$  and  $\beta_2 = 0$  and a learning rate of 0.05.

For the differentiable image transformations used in the parametric optimization, we utilized existing PyTorch implementations from Kornia [104], a differentiable library of classical computer vision algorithms. Additionally, we adapted some functions from the TensorFlow implementations of two GitHub repositories [53, 86].

For the style optimization, we used a high-resolution implementation of MUNIT provided by NVIDIA<sup>3</sup>.

## 6 EVALUATION OVERVIEW

While previous work has shown that image manipulation impact viewer emotions (see Sec. 2.3) and that strong user emotions boosts online engagement (see Sec. 2.1), it is unclear if the emotional properties of images can be altered in a targeted fashion to regulate the emotions users experience and through that reduce their duration of internet use. Our study aims to address this research gap by investigating the following two research questions:

**RQ1:** Can computational image adaptations effectively reduce emotional arousal and adjust experienced valence toward a neutral level while preserving image quality?

**RQ2:** Do lower arousal levels and a more neutral emotional valence lead to a decreased duration of engagement with a social media feed?

We choose social media as the context for this evaluation, as it is among the most widely used services on the Internet [30] and is commonly linked to high arousal and polarized emotional valence [32, 85].

To address our research questions, we first evaluate whether our approach satisfies the defined *criteria* from a technical perspective. We then conduct two empirical studies to assess their perceptual and behavioral effects: one examining changes in perceived arousal, valence, and visual quality, and a second evaluating their association with social media usage duration. Both behavioral studies were preregistered on OSF [39, 40].

## 7 TECHNICAL EVALUATION

The goal of the technical evaluation is to evaluate the effectiveness of our approach in relation to the defined *criteria*. Specifically, we evaluate whether the proposed methods achieve the intended changes in valence and arousal, as predicted by the regressor, while maintaining image quality (FID, KID) and fidelity to the original image (R1 loss). In addition, we examine whether these alterations cause changes in image properties in accordance with previous findings from related work. To conduct the experiment, we run different parameter configurations of our methods and baselines on the validation set of the COCO database [72].

### 7.1 Baselines

We compare our approaches against six baselines described below:

- **Original:** The original set of images without any modification or adaptation, serving as baseline against which all adaptation approaches are compared.

<sup>3</sup><https://github.com/NVlabs/imaginaire>

- **Grayscale:** The original images converted to grayscale, removing all color information. Grayscale is already deployed in mobile operating systems as a digital well-being feature (e.g., Android’s productivity mode, Apple’s color filters). It therefore represents the current state of the art and is included in all evaluations.
- **Manual:** A baseline in which static image transformations are applied using manually selected parameters. Parameter values were chosen through expert tuning on a subset of images with respect to the predefined *criteria*. Similar adjustments (e.g., color and saturation changes) are already supported by mobile operating systems. This baseline allows us to assess whether our low-level image adaptation approaches, parametric and style optimization, offer benefits beyond manual parameter selection.

To analyze the contributions of different components in our diffusion-based approach, we introduced three ablated versions of the method. The variants were proposed to identify the impact of individual components of our methodology:

- **CG (classifier guidance only):** This version employs the deterministic DPM multistep solver to invert an image [76]. Resampling is performed using only classifier guidance, without text conditioning. For this baseline, we use DPM instead of DDIM as our initial experiments have shown that it produces inverted images of higher quality without NTO (as CG is not text conditioned NTO cannot be applied).
- **NTO-instruct (instruction-guided resampling):** In this version, images are inverted using NTO and resampled with CFG only, without the use of CG. To guide resampling, the caption is extended with the sentence: “*The image should elicit low arousal and neutral valence in its viewers.*”
- **NTO-edit (resampling with refined captions):** This version applies NTO for image inversion and resampling with a modified caption. Original captions were refined using GPT-4 by removing emotionally charged words or phrases, yielding text that remains close to the original while ensuring a neutral tone.

For the diffusion-model-based approaches guided by text, we empirically found that a CFG scale of 2.0 provided the best results. This value offered an effective trade-off between introducing meaningful changes to the image and preserving fidelity to the original content. As textual input, we used the image captions provided by the COCO dataset.

Since the resolution of images in the COCO dataset is approximately 512×512, we utilized the Diffusers implementation of Stable Diffusion from Stability AI<sup>4</sup> as the backbone for the diffusion-model-based approaches in this experiment. Importantly, using a different backbone diffusion model than in the other experiments demonstrates that the proposed approach is agnostic to the underlying diffusion model.

RGDR, parametric optimization, and style optimization follow a dual-objective design: one objective preserves similarity between adapted and original images, and the other adjusts images to balance valence and reduce arousal. In this setup, the *similarity-preserving objective* is controlled by a fixed weight ( $w_1 = 1.0$  for parametric/style optimization, and  $w = 2.0$  for RGDR). The *emotional adaptation objective* is controlled by a variable weight ( $w_2 \in \{0.1, 0.3, 0.5, 0.7, 1.0\}$  for parametric/style optimization, and  $s \in \{0.05, 0.1, 0.2, 0.3, 0.4\}$  for RGDR and CG).

## 7.2 Metrics

The primary objective of this evaluation is to validate whether the proposed approaches satisfy the defined *criteria* in a technical sense. To this end, we used our ResNet50 regressor (Sec. 4.1) to estimate the valence (criterion i) and arousal of images (criterion ii). To technically evaluate image quality, we calculated the Kernel Inception Distance (KID) and the Frechet Inception Distance (FID), both of which are widely used metrics for assessing visual quality (criterion iii). We further quantified their resemblance to the original images using the L1 norm (criterion iv).

<sup>4</sup><https://huggingface.co/stabilityai/stable-diffusion-2-1-base>

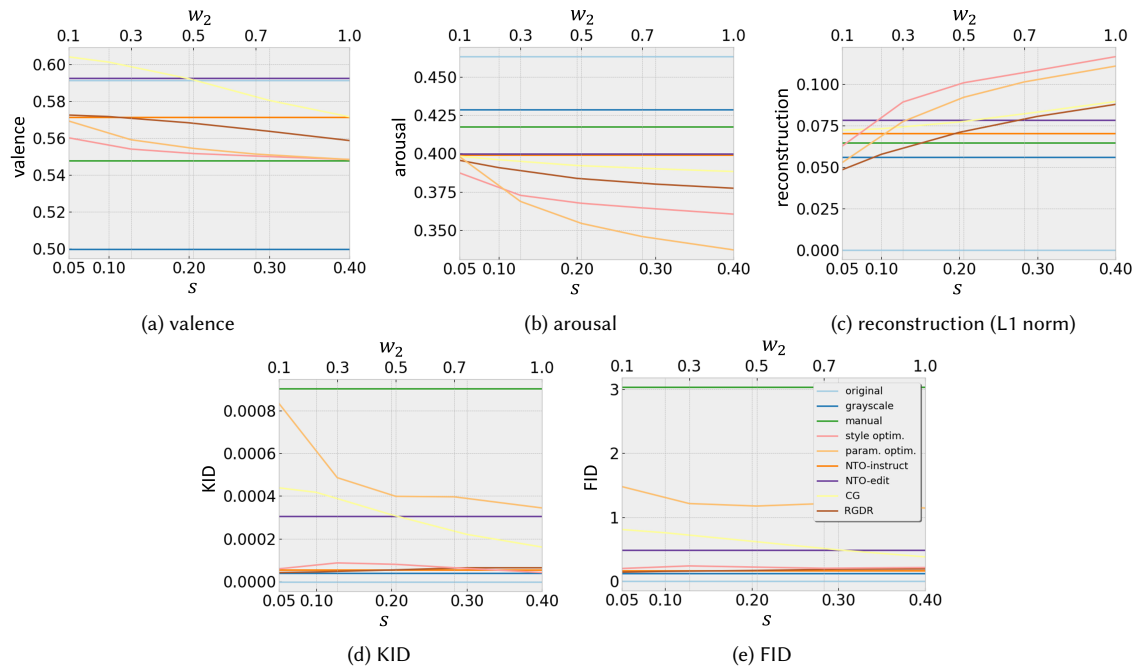


Fig. 5. Criteria alignment analysis: The plots show how the metrics evolve as the weighting of the objective terms that introduce emotional changes in the images increases. In each plot, the upper x-axis represents the values of  $w_2$  for parametric optimization and style optimization, while the lower x-axis indicates the values of  $s$  for RGDR and CG. The y-axes show the metric values.

Additionally, we quantified whether our approaches introduce changes to image properties in line with findings from previous research (Sec. 2.4). Thus, we measured the *colorfulness* and *saturation* of images using metrics proposed by Hasler and Suesstrunk [49]. The mean *brightness* of images was computed following the metric introduced by Goetschalckx et al. [43]. *Contrast* was calculated as described by Peli [95] and blur was assessed using the no-reference perceptual blur metric proposed by Crete et al. [26]. To quantify the *variability in edge orientations*, we followed the study by Redies et al. [102] and computed the first order entropy of edge orientations. To analyze *low-frequency changes in color and grayscale channels*, we computed Z-score transformed wavelet coefficients for both RGB and grayscale images using the methodology proposed by Delplanque et al. [33]. We quantified left-right mirror *symmetry* in images using the approach of Brachmann and Redies [14], leveraging filter responses of a convolutional neural network (VGG16) to capture color, edges, texture, and higher-order symmetry.

### 7.3 Results

We first present a quantitative analysis of whether the proposed approaches introduce changes to images according to our *criteria*. We then examine the qualitative implications of these changes, followed by an analysis of how the modified image properties align with previous research on their effects on emotionality.

*Criteria alignment.* Figure 5 illustrates how the metrics evolve as the weights of the emotional adaptation objective are adjusted. The results demonstrate that, in line with our *criteria*, all approaches effectively balance valence (Fig. 5a)

and lower arousal (Fig. 5b) compared to the original images. An exception is NTO-edit, which does not produce lower valence values relative to the original images.

To formally confirm this observation, we fitted ordinary least squares (OLS) regression models to the differences between the valence and arousal values of the original images and their adapted counterparts for each weight configuration of parametric optimization, style optimization, CG, and RGDR. For valence, the OLS models for all approaches were statistically significant ( $p < 0.03$ ), indicating that higher weights in the emotional adaptation objective were strongly associated with reductions in valence. The predictor term ( $\beta_1$ ) for each approach was as follows: style optimization ( $\beta_1 = -0.0121$ ,  $p = 0.022$ ), parametric optimization ( $\beta_1 = -0.0220$ ,  $p = 0.018$ ), CG ( $\beta_1 = -0.0960$ ,  $p < 0.001$ ), and RGDR ( $\beta_1 = -0.0401$ ,  $p = 0.001$ ). The observed negative relationships are attributable to the original images having a positive average valence, with increasing weight on the emotional adaptation objective driving them toward the *emotional reference*. For arousal, higher weights were consistently associated with reductions in arousal ( $p < 0.03$ ). The terms for each approach were as follows: style optimization ( $\beta_1 = -0.0274$ ,  $p = 0.027$ ), parametric optimization ( $\beta_1 = -0.0640$ ,  $p = 0.017$ ), CG ( $\beta_1 = -0.0282$ ,  $p = 0.003$ ), and RGDR ( $\beta_1 = -0.0513$ ,  $p = 0.005$ ).

As anticipated, the reconstruction error (Fig. 5c) increased with the rising weight of the emotional adaptation objective, reflecting the greater modifications introduced to the original images. Despite these changes, the low KID (Fig. 5d) and FID scores (Fig. 5e) across baselines and weights confirm that the adapted images maintain high visual quality.

*Qualitative findings.* Figures 6 and 7 provide examples illustrating how the different approaches adjust images to achieve the desired effect. RGDR introduces changes not only to colors but also to the content, often resulting in plastic transformations. For example, in Figure 6f, the man appears older, and in Figure 7f, the tram also ages as the weighting of the adaptation objective increases. Similarly, CG modifies both the color and content of images, however, artifacts can appear (Figure 6g). NTO-instruct and NTO-edit produce comparable adjustments, but their lack of consistency is evident in Figure 6d and 7e where they fail to adequately reduce valence and arousal to match the reference.

In contrast, style optimization and parametric optimization primarily alter the color values of images by introducing cooler tones (Figures 6i, 7h, 7i) or adding a red tint (Figure 6h). Similar changes are affected by manual (Figures 6c, 7c) Additional qualitative examples from this experiment are provided in Appendix D.

*Analyzing changes in emotional image properties.* We further examined whether RGDR, grayscale, style optimization, and parametric optimization altered emotional image properties relative to the original images in directions consistent with prior findings (Sec. 2.4). Whereas these studies analyze how image properties influence valence and arousal, we focus on the inverse: how adaptation methods guided by the *emotional reference* affect these properties.

*Brightness* is typically linked to positive valence [37, 113]. Given the slightly positive valence of the original images and the *emotional reference*, we expected brightness to decrease. This was observed for style optimization and parametric optimization, but not for grayscale or RGDR (Figure 8a).

Higher *saturation* has been associated with positive valence and arousal [103, 110], suggesting a reduction under the *emotional reference*. This was the case for grayscale and, to a lesser extent, RGDR, whereas style optimization and parametric optimization increased saturation (Figure 8b).

*Contrast* enhances valence when increased and reduces it when decreased [120]. Given the slightly positive valence of the originals, a slight reduction was expected and observed across all approaches (Figure 8c).

Studies indicate that colored images amplify both positive and negative valence and are more arousing than grayscale images [7, 21]. Accordingly, *colorfulness* was expected to decrease, which was observed across all approaches (Figure 8d).

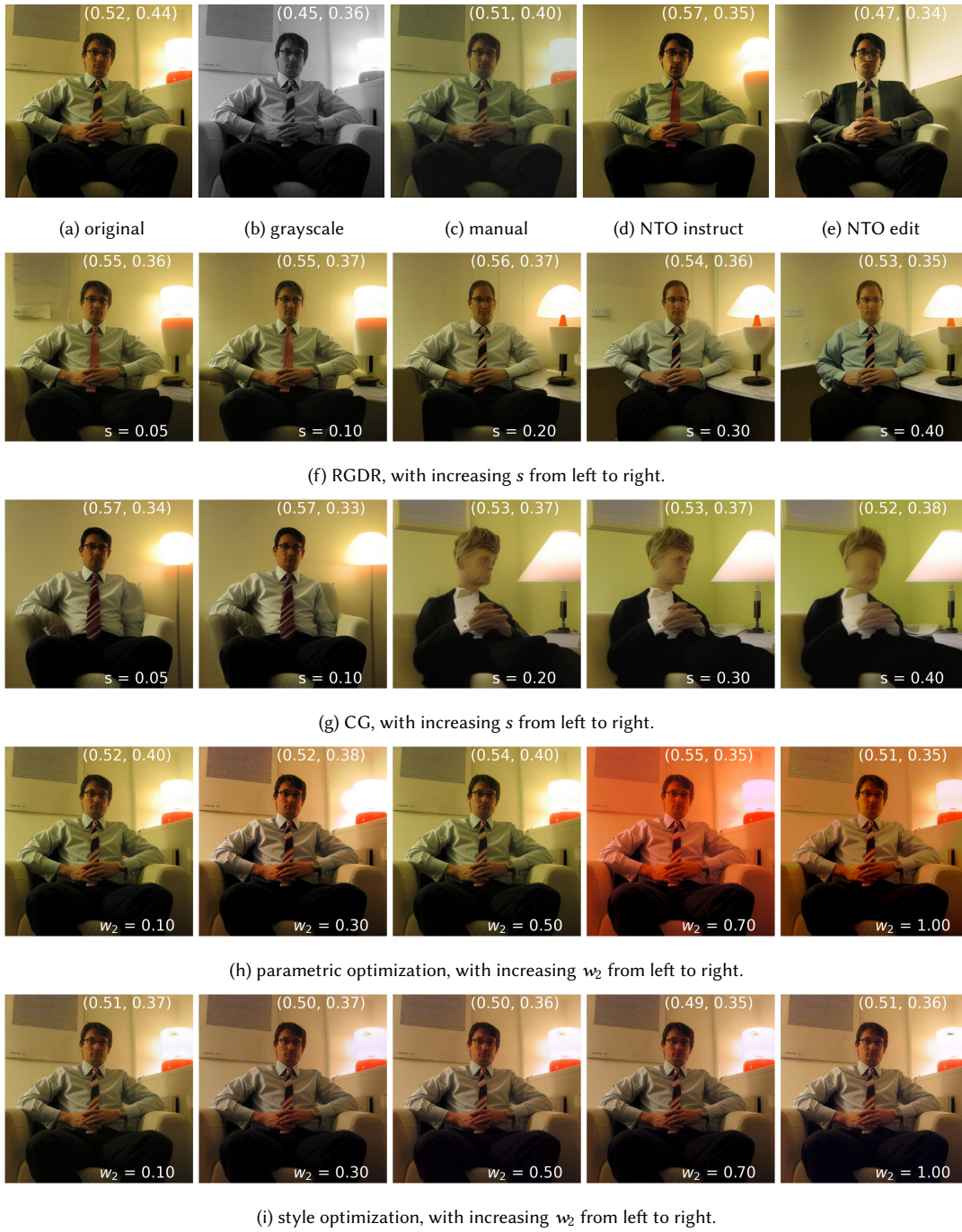


Fig. 6. Example result. Predicted valence–arousal values are shown top-right [target: (valence = 0.5, arousal = 0.0)].



Fig. 7. Example result. Predicted valence-arousal values are shown top-right [target: (valence = 0.5, arousal = 0.0)].

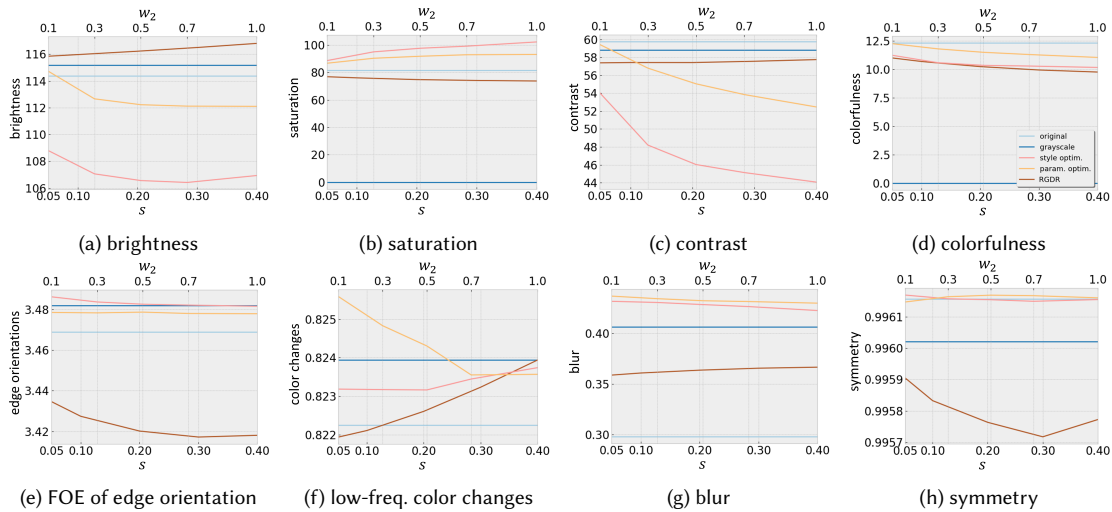


Fig. 8. Analyzing changes in image properties: The plots show how the metrics evolve as the weighting of the objective terms that introduce emotional changes in the images increases. In each plot, the upper x-axis represents the values of  $w_2$  for parametric optimization and style optimization, while the lower x-axis indicates the values of  $s$  for RGDR. The y-axes show the metric values.

Higher *1st-order entropy of edge orientations* corresponds to higher arousal [103]. As we aimed to reduce arousal, entropy was expected to decline, which was only true for RGDR (Figure 8e).

Images dominated by *low-frequency changes in color and luminance* are linked to higher arousal [33]. Contrary to expectations, all approaches showed slightly greater low-frequency changes than the originals, albeit with minor differences (Figure 8f).

*Blur* is known to reduce both valence and arousal [31]. As expected, all approaches increased blur (Figure 8g).

*Symmetry* is generally associated with higher valence and arousal [10–12, 15, 82]. Consistent with our *emotional reference*, RGDR and grayscale reduced symmetry, while style optimization and parametric optimization did not, though all differences were minor (Figure 8h).

## 7.4 Discussion

The technical evaluation demonstrates that the proposed approaches and baselines satisfy the defined *criteria* to varying extents. Our analysis shows that all examined approaches achieve KID and FID values indicative of high technical visual quality (criterion iii). Moreover, RGDR, style optimization, parametric optimization, and grayscale consistently produce image adaptations that move closer to the *emotional reference* than the remaining baselines (criteria i & ii). In contrast, the manual baseline reduces valence but fails to reliably lower arousal, indicating that low-level image adaptation benefits from per-image parameter optimization, as employed in the parametric and style-based approaches, rather than relying on static adjustments.

Ablation analyses further clarify the contribution of individual components in RGDR. Using classifier guidance alone (CG) moves both valence and arousal in the direction of the *emotional reference*, but less effectively than RGDR, and at the cost of stronger visual artifacts, as reflected in higher KID and FID scores, increased reconstruction error, and qualitative degradations (e.g., Fig. 6g). Editing the image caption and re-rendering the image using NTO (NTO-edit) reduces arousal but causes valence to deviate from the *emotional reference*, and yields slightly lower technical image quality than RGDR.

In contrast, the instruction-guided variant (NTO-instruct) preserves KID and FID values comparable to RGDR, but fails to steer valence and arousal toward the *emotional reference* to the same extent. Although RGDR achieves stronger emotional alignment at the cost of higher reconstruction error, a comparison of the corresponding trends (Fig. 5a,b vs. c) shows that these gains outweigh the associated cost. Overall, these results highlight that combining regressor-based conditioning with textual conditioning, as done in RGDR, enables more effective alignment with the *criteria* than relying on either CG or CFG alone.

When directly comparing RGDR with style optimization and parametric optimization, the latter two reduce arousal and valence more strongly according to the *emotional reference*, but this comes at the expense of substantially higher reconstruction error. However, also note that RGDR did occasionally introduce visible artifacts, particularly around the extremities of human subjects (see Sec. 10.2 for further discussion). Importantly, all three approaches allow a flexible trade-off between emotional alignment (criteria i & ii) and fidelity to the original image (criterion iv), outperforming both low-level adaptation baselines and diffusion-based ablations that omit one of the two conditioning signals.

We further examined if adaptations produced by grayscale, RGDR, style and parametric optimization align with prior findings on emotional image properties. All approaches exhibited changes in *contrast*, *colorfulness*, and *blur* consistent with theoretical expectations. In addition, style optimization and parametric optimization behaved as expected with respect to *brightness*. By contrast, grayscale and RGDR matched expectations for *saturation*, with RGDR being the only approach that fulfilled expectations for the *first-order entropy of edge orientations*. Other properties, including *low-frequency color changes* and *symmetry*, showed only minor deviations from the original images across all approaches.

Finally, we assessed the robustness of the proposed approaches by varying the optimization objective to target alternative emotional references within the CMA space (e.g., high valence and high arousal). The methods produced meaningful changes in response to different emotional references. Results are provided in Appendix C.

In summary, our technical evaluation demonstrates that our three proposed approaches modify image properties in the direction of the *emotional reference* and satisfy the defined *criteria* more effectively than the baselines (with the exception of grayscale). While style optimization and parametric optimization primarily achieve this through low-level adjustments (e.g., color and contrast changes), RGDR enables semantic modifications (e.g., increasing the apparent age).

To examine whether these technical effects translate into perceptual outcomes, we next evaluate the adapted images in a controlled image-rating experiment, comparing RGDR, style optimization, and parametric optimization against original and grayscale images.

## 8 IMAGE RATING STUDY

This study evaluates whether our approaches reduce perceived emotional arousal and balance perceived valence while maintaining high perceived image quality (**RQ1**). We compare the adapted images against the original images and the grayscale baseline introduced earlier as the current state of the art.

### 8.1 Study design

In the following, we detail conditions, stimuli, task and participants of the experiment.

*Stimuli.* The stimuli we used in this study stem from the Nencki Affective Picture System (NAPS) [84]. It consists of 1,356 realistic, high-quality photographs for which affective ratings were collected from 204 participants. They are divided into five categories: people, faces, animals, objects, and landscapes. We selected images from the categories of people, faces, animals, and landscapes as they represent genres frequently seen on social media [68].

Following the approach of Mould et al. [91], we divided the valence-arousal space into distinct regions. We excluded regions that are positioned near the optimization target (low arousal/neutral valence) as for images in these regions the adaptations are minimal by design. The final image selection was drawn from four clusters: mid arousal/low valence, high arousal/low valence, mid arousal/high valence, and high arousal/high valence (see Figure 9). From each cluster, we selected three images, resulting in a total of 12 stimuli. In addition, we sampled 5 images from the whole valence arousal spectrum to show in the calibration phase of the experiment. As the usage rights of NAPS prohibit publishing its images, the stimuli are not displayed here.

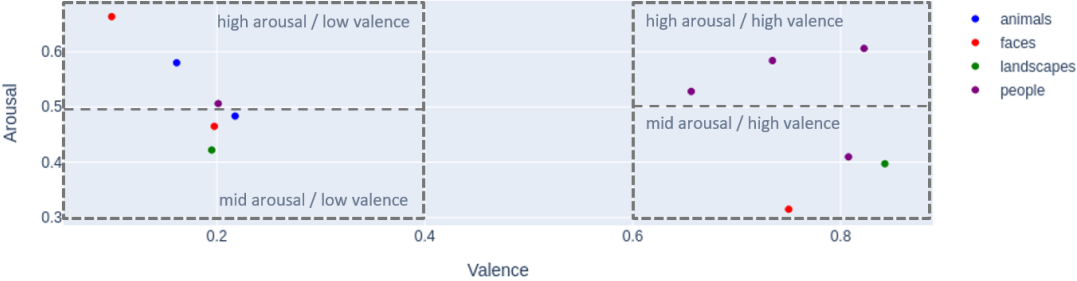


Fig. 9. Location of selected stimuli within the valence arousal space of the Circumplex Model of Affect [106]. To select images from a spectrum of valence and arousal values, they were drawn from four clusters: mid arousal/low valence, high arousal/low valence, mid arousal/high valence, and high arousal/high valence.

The 12 images form a block, presented in each condition. For the order within each block, we followed the study design of Mould et al. [91], starting and ending with lower-arousal, positive images to ease participants into the new technique and leave them with a positive sentiment. Specifically, we began and concluded each block with images from the mid arousal/high valence cluster, then proceeded counterclockwise through the specified clusters in the valence-arousal space.

*Task.* Participants were asked to observe an emotional image for a minimum of five seconds. After these five seconds, participants could choose to either continue viewing the image or proceed with the experiment by pressing the space key on their keyboard. The total viewing duration was recorded as observation time. Following that, participants were directed to the next webpage, where they were asked to complete a validated questionnaire, which collects emotional valence and arousal ratings [16]. Additionally, they were asked to rate a Likert item assessing the quality of the image (adjusted from [91]). To prevent emotional contamination between images, we showed a neutral stimulus after each image-questionnaire pair. The task was repeated for all 12 images in each condition.

*Conditions.* The study conditions included images adapted with RGDR, the style optimization and parametric optimization, along with the images in their original form and after applying a grayscale filter. Based on the results of our technical evaluation and additional empirical tests, we selected the adaptation weights to balance the trade-off between reducing evoked emotions and maintaining fidelity to the original images. The weights for each approach were RGDR:  $w = 2.0, s = 0.2$ ; style optimization:  $w_1 = 1.0, w_2 = 0.2$ ; parametric optimization:  $w_1 = 1.0, w_2 = 0.15$ .

Following the experimental setup of preceding studies [13, 91], the study contains one within-subject factor (IMAGE ADAPTATION TECHNIQUE) with 5 factor levels (*original, grayscale, RGDR, style opt., param. opt.*). With each adaptation approach, we adapted the block of images. Each block was presented to participants with a fixed order of images. To avoid order effects, we used latin-square counterbalancing to adjust the order of blocks between participants.

*Procedure.* Participants first signed a consent form and completed a demographic questionnaire. They then viewed a brief study introduction and familiarized themselves with the setup using a trial run featuring a placeholder image. Following a two-minute relaxation video, participants received on-screen instructions to start the experiment. The experiment involved sequential exposure to calibration images followed by five blocks of images per condition (see *Stimuli* for details), with self-assessments after each image. Upon completion, participants received a code to claim a monetary reward of £4.5. The study took approximately 30 minutes per participant.

*Participants.* We conducted an a priori power analysis to establish the minimum sample size needed to test our hypotheses. To achieve 95% statistical power at  $\alpha = 0.05$  for a repeated-measures ANOVA with five conditions and a Cohen's  $f$  of 0.2, we estimated a required sample size of  $N = 48$ . The chosen effect size was based on reported values in similar studies (0.25–1.5; [7, 31]). To account for potential outliers or participants who might not complete the study faithfully, we recruited 59 participants (33 female, 26 male), ages 18–74 ( $M=36$ ,  $SD=11.5$ ) from the online crowd-sourcing platform Prolific. We excluded three participants whose data clearly indicated they did not perform the task faithfully (e.g., rating all images identically or producing patterned responses). The data of the remaining 56 participants was used in the analysis. Importantly, the significance of the results remains unchanged regardless of whether these outliers were included or excluded.

## 8.2 Results

In the following, we present the results of the study. For significance testing, we conducted an ANOVA with sphericity corrections applied to all within-subject factors. Notably, the significance of the results remain consistent regardless of whether the sphericity correction is applied. Post-hoc pairwise comparisons were performed using t-tests without correction, as they served to assess a pre-registered, directional hypothesis regarding the effects of image adaptations on emotional arousal, valence, and image quality [40]. According to the hypothesis, pairwise comparisons are conducted exclusively between each condition and the original images. Figure 10 shows an overview of the study results.

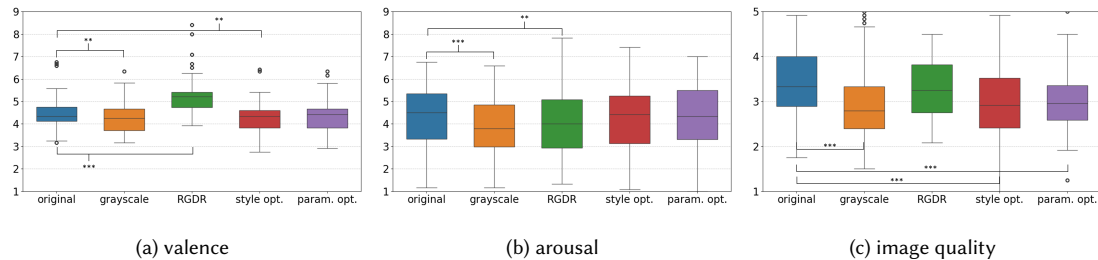


Fig. 10. Results of behavioral study: Boxplots of subjective ratings of participants for valence (a), arousal (b), and image quality (c). Consistent with the preregistered hypothesis, only significant differences compared to the original images are indicated (\*  $p < 0.05$ , \*\*  $p < 0.01$ , and \*\*\*  $p < 0.001$ ). The box represents the interquartile range (IQR; Q1–Q3), the central line marks the median, and the whiskers extend to the smallest and largest values within  $1.5 \times$  IQR, with points beyond plotted as outliers. The y-axes show Likert response levels of the respective item.

We found an effect of the IMAGE ADAPTATION TECHNIQUE factor levels on valence ratings [ $F(2.80, 153.84) = 69.32$ ,  $p < .001$ ,  $\eta_p^2 = .56$ ]. Post-hoc pairwise comparisons showed that *RGDR* was associated with an increase in valence ratings relative to *original* ( $p < .0001$ ,  $d = 1.51$ ), whereas *style opt.* ( $p < .003$ ,  $d = 0.42$ ) and *grayscale* ( $p < .003$ ,  $d = 0.43$ ) showed reductions. No other conditions differed significantly from *original* in valence.

Because the reference point for valence optimization corresponds to the midpoint of the Likert scale (5), rather than zero, we conducted exploratory one-sample t-tests comparing mean valence ratings for each condition against this midpoint. Valence ratings for both *original* and *grayscale* differed from 5 (*original*: [ $t(55) = -5.55, p < .001, d = .74$ ]; *grayscale*: [ $t(55) = -8.97, p < .001, d = 1.2$ ]). Similarly, *style opt.* and parametric optimization also showed deviations from the midpoint (*style opt.*: [ $t(55) = -7.86, p < .001, d = 1.05$ ]; parametric optimization: [ $t(55) = -7.39, p < .001, d = 0.99$ ]). In contrast, only RGDR did not differ from the neutral midpoint [ $t(55) = 1.91, p = .062$ ].

In addition, the ANOVA showed that there was an effect of the IMAGE ADAPTATION TECHNIQUE on arousal ratings [ $F(3.24, 178.08) = 7.79, p < .001, \eta_p^2 = .12$ ]. Post-hoc tests showed that RGDR ( $p < .002, d = .45$ ) and *grayscale* ( $p < .0001, d = .68$ ) both caused lower arousal ratings than default. No other arousal differences were observed relative to *original*.

Exploratorily, we further conducted pairwise comparisons between conditions and *grayscale*. These revealed that *grayscale* elicited lower arousal ratings than both *style opt.* ( $p < .001, d = .56$ ) and *param. opt.* ( $p < .001, d = .52$ ), while no differences between *grayscale* and RGDR were found.

The ANOVA also revealed a main effect of IMAGE ADAPTATION TECHNIQUE on perceived image quality [ $F(2.73, 150.19) = 10.04, p < .001, \eta_p^2 = .15$ ]. Pairwise comparisons showed that *grayscale* ( $p < .0001, d = .71$ ), *param. opt.* ( $p < .0001, d = .64$ ), and *style opt.* ( $p < .0001, d = .72$ ) were associated with lower image quality ratings than *original*. In contrast, RGDR did not differ from *original* [ $t(55) = 1.75, p = .09$ ].

No significant difference was found in the case of observation time.

### 8.3 Discussion

Our experiment tested whether the manipulations in each condition altered viewers' perceived valence, arousal, and image quality relative to *original*. For valence, *grayscale*, *style opt.*, and RGDR differed from *original*, but only RGDR increased ratings toward the *emotional reference* of the image optimizations (equivalent to 5 on the Likert scale). Consistently, RGDR was the only condition showing no difference from this neutral midpoint. For arousal, RGDR and *grayscale* yielded lower ratings than *original*, whereas *param. opt.* and *style opt.* did not. No difference between RGDR and *grayscale* indicates that both conditions reduce arousal to a similar extent. However, in contrast to *grayscale*, RGDR did not result in a significant reduction in perceived image quality relative to *original*. This indicates that RGDR is the only condition that successfully shifts emotional perception without compromising perceived image quality, and thus the only approach that fully addresses **RQ1**.

To examine whether these perceptual effects translate into behavioral outcomes, we next evaluate whether the adapted images influence browsing behavior, comparing RGDR against original and grayscale images. We exclude *param. opt.* and *style opt.* from this analysis, as they did not satisfy the criteria required to address **RQ1**.

## 9 SOCIAL MEDIA STUDY

This study examines the impact of RGDR on internet behavior, specifically whether emotionally adapted images reduce the time users spend browsing a social media feed (**RQ2**). We compare the adapted images against the original images and the grayscale baseline.

### 9.1 Study design

In the following, we detail conditions, stimuli, task and participants of the study.

*Stimuli.* To ensure the external validity of our study, we used real social media posts, including both text and images, as stimuli. Specifically, we used posts from the Instagram Influencer Dataset [62]. It contains of 10,180,500 Instagram posts from 33,935 influencers. Each post consists of its metadata and associated image files. Posts are classified into the following nine categories: beauty, family, fashion, fitness, food, interior, pet, and travel. To match preferences of a broader audience, we chose posts from the categories fitness and travel.

To generate experimental stimuli, we randomly sampled 812 images from posts in the target categories. Each image was processed eight times with our algorithm to account for quality variations in diffusion-generated images (discussed in Sec. 10), and an annotator selected the best version. Images with artifacts in all versions (47 in total) were discarded, leaving 765 images. Because many predicted valence and arousal values were already close to the *emotional reference*, not all images showed changes relative to their originals. A second manual review was therefore conducted, as regressor-based predictions did not yield a clear decision boundary. This review identified 268 altered images, which were used in the first feed across all conditions, either in their original form, in grayscale, or as adapted by our approach.

We computed the order of posts using the quadrant based approach of the image rating study. However, as valence and arousal values of images are distributed differently, we computed the 2D center of mass for valence and arousal of all images of the posts, then based on the center defines four quadrants around them. We then created the feed by sampling from the quadrants such that the first element is randomly drawn from Q1, the second element is randomly drawn from Q2, then Q3 and Q4, until all posts are part of the feed. This ensures that the emotions that the images in the feed elicit are distributed similarly across the feed.

*Task.* Participants browsed two curated social media feeds in sequence. Participants began by browsing the first social media feed that contained images adjusted according to one of the conditions. After 30 seconds, a button to access the second feed (with unadjusted images) became available. Upon clicking this button, participants evaluated the quality of the first feed’s images and completed emotional self-reports [16]. They then proceeded to the second feed. The study was automatically terminated such that participants spent five minutes browsing the feeds. Before the main task, participants completed a guided trial run to familiarize themselves with the procedure.

*Conditions.* The study included three conditions: original images, grayscale images, and images adapted with RGDR. We included RGDR because it was the only approach that fully addressed **RQ1**. Grayscale images were included as a baseline, as grayscaling is already deployed in mobile operating systems as a digital well-being feature.

It followed a between-subjects design with a single factor (*IMAGE ADAPTATION TECHNIQUE*) with 3 factor levels (*original, grayscale, RGDR*). Factor levels varied between participants, who were randomly assigned using a block randomization approach. All images in the first social media feed were adapted according to the respective factor level. The weights for RGDR were the same as in the image rating study:  $w = 2.0$ ,  $s = 0.2$ .

*Procedure.* After providing informed consent and completing a demographic questionnaire, participants received a brief study introduction and completed a one-minute practice task featuring comic animal images instead of social media content. A two-minute relaxation video preceded the main task. Participants then engaged with the first social media feed. After 30 seconds, they were allowed to switch to a second feed or continue browsing the first feed for up to five minutes. Switching feeds or reaching the five-minute limit triggered a questionnaire comprising the same Likert-scale items used in the image rating study (perceived arousal, valence, and image quality), as well as comprehension and attention checks. If less than five minutes had elapsed, participants were subsequently shown the second feed for the

remaining time. Upon completion of the study, participants received a code to claim a £2.25 reward. The study lasted approximately 15 minutes.

*Participants.* A priori power analysis indicated that a sample size of  $N = 159$  would be required to achieve 80% power to detect an effect of Cohen's  $f = 0.25$  at a significance level of  $\alpha = .05$  in a fixed-effect, omnibus one-way ANOVA with three factor levels (original, grayscale, and our image-editing approach). The chosen effect size was based on values reported in similar studies ( $f = 0.25-1.5$ ; [7, 31]). For post-hoc tests between image adaptation techniques, we conservatively planned conducting two-tailed independent-samples t-tests, despite having preregistered directional hypotheses [39]. Assuming an effect size of Cohen's  $d = 0.5$  ( $f = 0.25$ ) and  $\alpha = .05$ , a sample of  $N = 128$  ( $n = 64$  per group) would provide 80% power. Adopting a more conservative approach, we based our target sample size on the pairwise comparison analysis, resulting in a required total of  $N = 192$  participants (three conditions  $\times$  64 participants).

We recruited participants via Prolific, prescreening for active social media users. Individuals who failed an attention check were replaced without their data being examined. In total, 216 people were recruited to achieve the target sample size of 192. Of these, four were excluded for not interacting with the feeds ( $n = 3$ ) or due to technical issues ( $n = 1$ ). The final sample consisted of 188 individuals (91 female, 96 male, 1 non-binary), aged 19–75 years ( $M = 38$ ,  $SD = 11.5$ ). On average, participants reported spending 3.5 hours per day on social media ( $SD = 2.5$ ; range = 0.5–15).

## 9.2 Results

We first report the statistical analysis of the behavioral data, followed by qualitative observations on the types of edits introduced to social media images by our approach.

*Analysis of behavioral data.* To analyze the behavioral data, significance testing was conducted using ANOVA with sphericity corrections applied to the three between-subject factors. Importantly, the pattern of significant results was consistent irrespective of whether the sphericity correction was applied. Post-hoc pairwise comparisons were performed using t-tests without correction, as these analyses addressed pre-registered directional hypotheses concerning the effects of image adaptations on emotional arousal, valence, image quality, and the time participants spent in a social media feed [39]. According to these hypotheses, pairwise comparisons are conducted exclusively between each condition and the original images. Figure 11 shows an overview of the results of the study.

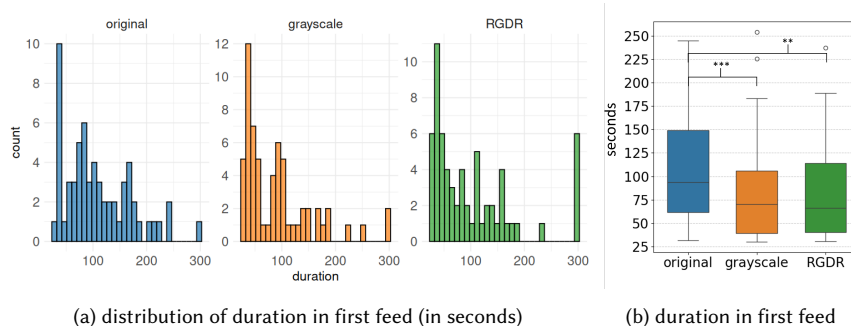


Fig. 11. Results of social media study: (a) Histogram depicting the distribution of durations participants spent in the first feed. (b) Boxplots illustrating durations spent in the first feed, with significant differences relative to the original images indicated (\*  $p < 0.05$ , \*\*  $p < 0.01$ , and \*\*\*  $p < 0.001$ ). In a boxplot, the box represents the interquartile range (IQR;  $Q1-Q3$ ), the central line marks the median, and the whiskers extend to the smallest and largest values within  $1.5 \times$  IQR, with points beyond plotted as outliers.

We first analyzed responses to a comprehension check (“The experiment allowed me to switch from the first to the second feed (after the button was active).” - correct answer: yes). Participants who answered correctly ( $N = 149$ ) were compared with those who did not ( $N = 39$ ). A Pearson’s chi-squared test with a simulated p-value (100,000 replicates) showed no association between comprehension accuracy and whether participants switched feeds [ $Z = 0.53, p = 0.69$ ]. A Welch’s two-sample t-test likewise revealed no difference in time spent in the first feed between groups [ $t(61.08) = 0.38, p = .7062$ ]. We therefore concluded that comprehension check performance had no effect on participant behavior and included all participants in subsequent analyses.

Inspection of the distributions (Figure 11a) revealed that nine participants remained on the first feed for the entire task duration of 300 s (*grayscale*:  $n = 2$ ; *RGDR*:  $n = 6$ ; *original*:  $n = 1$ ). As this behavior contradicted the study instructions, it likely indicates reduced engagement or distraction by other tasks. Consequently, we excluded these nine participants from further analyses, leaving 179 participants in the final dataset.<sup>5</sup>

A main effect of the IMAGE ADAPTATION TECHNIQUE on time spent in the first feed was observed, [ $F(2, 174) = 3.76, p = .025, \eta_p^2 = .04$ ]. Post-hoc comparisons showed that both *RGDR* ( $p = .024, d = .41$ ) and *grayscale* ( $p = .003, d = .39$ ) reduced time spent in the first feed relative to *original*. An exploratory post-hoc comparison revealed no difference between *RGDR* and *grayscale* ( $p = .92$ ). No other differences relative to *original* were observed for any variable.

In addition to the preregistered analyses, exploratory one-sample t-tests compared mean valence ratings for each condition against the neutral midpoint of the valence scale (5), which served as the optimization reference. Ratings for *original* were different than the midpoint [ $t(60) = 2.21, p = .031, d = .28$ ], whereas ratings for both *RGDR* and *grayscale* did not differ significantly from 5.

*Analysis of adapted social media images.* We also conducted a qualitative inspection of the social media images adapted by our approach. The results, presented in Figure 12, demonstrate that our method introduces meaningful semantic modifications to align the images with the defined *emotional reference*. Commonly observed changes include making subjects appear older (Figure 12a), less attractive (Figure 12b), adding layers of clothing (Figure 12c), or altering facial expressions (Figure 12d). Additionally, *RGDR* may remove subjects from images (Figure 12e), reduce their size (Figure 12f), make animals appear less cute (Figure 12g), or simplify the background (Figure 12h). Further qualitative results demonstrating these patterns can be found in Appendix E.2.

### 9.3 Discussion

The results indicate that both *RGDR* and *grayscale* were associated with reduced time spent in the first social media feed, with no evidence of a difference between them. No significant differences were observed for perceived arousal or image quality. However, we found that valence ratings in the *original* condition were significantly higher than the neutral midpoint, whereas ratings for *RGDR* and *grayscale* did not differ from it. For *RGDR*, this is consistent with the optimization target of neutral valence.

Qualitative analysis provides additional insight into this pattern. Images adapted using *RGDR* exhibited semantic changes such as making subjects appear older or less attractive, altering facial expressions, adding clothing, reducing subject prominence, or simplifying backgrounds. Collectively, these changes are consistent with theoretical accounts of how high-level content features influence emotional responses (e.g., nudity increasing arousal or attractiveness eliciting positive emotions; see Sec. 2.4), and suggest that *RGDR* shifted image content toward the defined *emotional reference*.

<sup>5</sup>Notably, including the nine participants in the analysis of time spent in the first feed revealed no differences between conditions.



(a) Subjects get older. Caption: "The woman in a pink dress holding her belly with the man in a blue t-shirt."



(b) Subjects decline in attractiveness. Caption: "A blonde woman poses in black ripped jeans and black top."



(c) Subjects get clothed. Caption: "A shirtless man holding a cup, sitting on a bed with a scenic mountain view."



(d) Subjects' facial expression is changed. Caption: "Woman practicing yoga in a modern kitchen."



(e) Subjects get removed. Caption: "Woman lying on a wooden deck above a calm water surface during a sunset."



(f) Subjects are reduced in size. Caption: "Surfer riding a large ocean wave with people in the background."



(g) Animals appear less cute. Caption: "A small dog sitting on a bed inside a camper van with mountains visible through the front window."



(h) Background becomes simpler. Caption: "Person sitting under a tree gazing at the starry night sky with the Milky Way visible in the background."

Fig. 12. Social media images adapted with RGDR, each illustrating a typical change it induces (see sub-caption).

Taken together, while both *RGDR* and *grayscale* were associated with reduced browsing duration and valence ratings closer to neutrality, no corresponding reduction in perceived arousal was observed. This prevents a conclusive answer to **RQ2**. Nevertheless, the convergence of reduced engagement and emotionally balanced valence suggests a potential association between emotional modulation and browsing behavior, motivating further investigation of emotional mechanisms using designs with greater sensitivity to arousal effects (see Sec. 10 for further discussion).

Importantly, the image-rating study (Sec. 8) reveals a key distinction between the two approaches: while *grayscale* led to a significant degradation in perceived image quality relative to the original images, *RGDR* achieved comparable emotional and behavioral effects without compromising visual quality. This positions *RGDR* as a more promising alternative for reducing time spent online while preserving users' visual experience.

## 10 LIMITATIONS & FUTURE WORK

While our findings provide valuable insights, they remain preliminary. In the following, we discuss limitations and potential directions for future research, focusing on study design, method, ethical implications, and real-world use.

### 10.1 Study design

Several aspects of our study design limit its internal and external validity.

*10.1.1 Internal validity.* In the social media study, we did not observe significant differences in self-reported image quality or arousal, which prevents a conclusive answer to **RQ2**. Detecting differences in self-reported attitudinal measures is particularly challenging in between-subject designs due to substantial inter-individual variability, with such effects often more reliably detected in within-subject paradigms [7, 31]. We deliberately opted against a within-subject design, as pre-studies indicated that repeated exposure to the same feed led to familiarity effects, while varying feeds across conditions introduced content-related confounds that could not be controlled. As a result, potential differences in perceived arousal or visual quality may have remained undetected.

Future work should explore study designs that better control for inter-individual variability (e.g., longitudinal or hybrid designs) to improve sensitivity to changes in self-reported attitudinal responses.

*10.1.2 External validity.* Several aspects of our study design limit its external validity, as our method is not yet capable of adapting internet content in real time. First, because images had to be preprocessed, the study was conducted using a curated social media feed. While this improved internal validity by ensuring that all participants viewed the same content, it did not reflect the personalized nature of real social media feeds and may therefore have elicited less natural user behavior. Moreover, the controlled setting, in which participants were observed and used social media for a fixed period, differs from naturalistic use and likely influenced behavior.

Second, we attempted to approximate real-world internet use by including the possibility of switching to an alternative task competing for users' attention. To minimize interpersonal variation in perceived task value, we used a second social media feed rather than an unrelated activity. However, this does not reflect the diverse range of alternative activities available in everyday contexts and may have influenced participants' disengagement decisions.

Third, both studies were conducted under time constraints acceptable to participants. To ensure measurable effects within the available time frame and number of stimuli, we deliberately selected images likely to elicit strong emotional responses: in the image-rating study based on pre-labeled valence and arousal values from emotional image databases, and in the social media study through manual selection of images that deviated noticeably from their originals and the

emotional reference targeted by our approach. In contrast, real-world social media content is often more emotionally neutral and consumed over longer periods, which may lead to engagement dynamics not captured in our study.

Future research should examine whether our findings hold in realistic online environments, where original social media content is used, user behavior is natural, and emotional exposure occurs over longer time spans.

## 10.2 Method

Our method inherits common limitations of diffusion-based image generation, including variability in output quality and difficulties in accurately depicting human limbs. These challenges remain an active research area.

In addition, our approach introduces emotional changes through CG by backpropagating gradients directly to the predicted noise during denoising. In practice, this can lead to unstable image synthesis, as gradients derived from the classifier may conflict with those induced by textual conditioning. Existing diffusion-based methods rely on attention-based regressor guidance to solve this issue, however, this can introduce perceptual artifacts (e.g., oversaturation) that conflict with our goal of emotionally neutral, low-arousal images (see Sec. 2.3.3 for a detailed discussion). Future research should thus explore mechanisms that enable emotional image adaptation via classifier guidance while better aligning CG gradients with those of CFG to ensure stable synthesis and perceptually balanced results.

In parallel, OpenAI and Google have introduced autoregressive multimodal models (GPT-4o, Nano Banana Pro), which demonstrate unprecedented text-based image editing capabilities through a transformer-based architecture [45, 56]. An interesting direction for future work is to explore whether these models can enable text-driven image editing that modulates emotional responses, which diffusion models in our experiments failed to accomplish reliably.

Another limitation of our method is its runtime, which is not yet suitable for real-time use (90 s per image on average). Accelerating diffusion models is an active research direction, with recent work demonstrating near-real-time inference speed [23, 112]. Beyond images, online content consists of text and, in particular, video. Extending our approach to these modalities is a natural next step. Text could be adapted using LLM models, while videos could be modified by adapting our approach to video diffusion models [52].

## 10.3 Ethical implications

Our research raises ethical concerns, as it subtly alters images to influence users' emotions and behavior. Moreover, modifying visual content may be perceived as a form of censorship, particularly if certain types of content are systematically attenuated. For deployment in consumer-facing systems, it is therefore essential that such interventions are explicitly initiated by users, aligned with their personal goals, and transparently communicated. Ensuring user awareness and control is critical to maintaining trust and supporting ethical behavior change.

A further concern is that our approaches alter content in ways that may override the original intent and expressive choices of content creators. Creators already make deliberate use of tools, such as beautification filters, to amplify emotional appeal and maximize engagement, mechanisms that have contributed to the prevalence of highly emotional content on social media. In contrast, our work shifts agency toward the consumer by enabling users to decide the degree of emotional intensity they wish to encounter. This raises an important ethical question: to what extent is it acceptable to modify content presentation when such modification is explicitly chosen by users to manage emotional overload in an online environment emotionally optimized to maximize engagement [118]?

RGDR may also replicate biases present in its training data, including stereotypes related to gender, skin tone, or other socially salient attributes. Future work should address these risks through the curation of balanced, representative datasets reflecting diverse populations and social norms, alongside systematic fairness evaluations.

Finally, the proposed approaches could, in principle, be repurposed to optimize images toward other emotional targets, including states that may be manipulative or harmful. Importantly, this risk is not unique to our methods, as the underlying architectures build entirely on existing models and techniques. Rather than introducing a fundamentally new capability, our work makes explicit how readily emotional image adaptation can be realized. We argue that such transparency is ethically important, as it can support informed debate and the development of norms and safeguards around emotion-aware content adaptation.

#### 10.4 Real-world use

In addition to the technical and ethical challenges outlined above, our method faces further obstacles to real-world application. A key concern arises in the context of personalized social media feeds: how should images be adapted when they depict familiar individuals, such as friends or family members? One possible strategy would be to detect such images and exclude them from adaptation. Given that personal relevance strongly shapes emotional responses [55, 97], addressing this issue is critical for the practical application of emotion-regulating image adaptation.

While the strength of the emotional modifications introduced by RGDR is parameterizable via the weighting of content preservation ( $w$ ) and emotional guidance ( $s$ ), we selected these parameters to ensure that the induced changes were sufficiently pronounced to be perceptually detectable within the constraints of our experimental design. In real-world deployments, however, more subtle modifications may be sufficient to influence engagement. Identifying appropriate parameter settings could be explored through user-centered studies (e.g., JNI-style iterative evaluations) or, more dynamically, through closed-loop systems that continuously assess user state and goals and adapt intervention intensity over time. Future research should examine how adaptive tuning strategies can support effective behavior change while inducing only minimal changes to image appearance.

Prior work on digital self-control tools has shown that implicit input manipulations can reduce usage time [77], aligning with the principle that effective interventions should avoid overt coercion [79]. However, such approaches typically achieve reduced engagement at the cost of mild frustration or degraded interaction quality. In contrast, although computationally more demanding, our approach does not rely on inducing negative affect. Instead, it adapts visual content to elicit emotionally neutral responses while preserving image quality, content fidelity, and the integrity of user interaction, thereby supporting natural disengagement without undermining user autonomy.

#### 10.5 Negative social comparison

In contrast to existing DSCTs, we believe our method may benefit social media users beyond restoring agency over the time they spend on platforms. An interesting direction for future research is to investigate whether the adapted images generated by our method can reduce the tendency for negative social comparisons. Social media often emphasizes aspirational aspects of life, such as luxury, beauty, and happiness, which can create a stark contrast to users' everyday experiences. These feelings of inadequacy often trigger negative emotions like dissatisfaction, envy [32], and anxiety [2]. These emotional responses can spiral into severe mental health issues such as depression [70], suicidal thoughts [2], and anorexia [114], particularly among younger users. We hypothesize that more neutral, less arousing images could reduce negative social comparisons, potentially leading to fewer feelings of inadequacy and alleviating related symptoms.

## 11 CONCLUSION

This paper examined whether modifying the emotional properties of images can support non-coercive reductions in time spent online. Building on prior work linking emotional arousal and valence to online engagement, we introduced

and systematically analyzed three regressor-guided image adaptation approaches that operate at different levels of visual abstraction to modulate the emotions elicited by images: parametric optimization, style optimization, and RGDR.

The parametric optimization approach modifies low-level image properties such as color, brightness, and contrast through differentiable global transformations. Operating at a similar level of visual abstraction, the style optimization approach optimizes a latent style representation while preserving the underlying image content. In contrast, the diffusion-based approach, RGDR, enables high-level semantic adaptations by steering the generative process using emotional guidance, allowing for subtle changes in content such as facial expression, apparent age, attractiveness or degree of nudity. This progression from low-level to high-level control enabled a systematic comparison of how different forms of image adaptation affect emotional perception and user behavior.

Across a technical evaluation, a controlled image-rating study, and a social media experiment, we found that while all three approaches can technically steer images toward a target of neutral valence and low arousal, only RGDR altered perceived emotions without degrading perceived visual quality. In a simulated social media environment, images adapted using RGDR were associated with reduced browsing duration, indicating that high-level emotional content modulation may influence online usage behavior in the absence of enforced restrictions. Notably, unlike grayscale-based interventions, already deployed in mobile operating systems as digital well-being features, RGDR achieved these effects while preserving visual quality. Together, these results position diffusion-based emotional image adaptation as a promising alternative to existing digital well-being strategies.

More broadly, this work contributes a systematic evaluation of emotion-aware image-editing strategies and highlights a new design space for digital well-being interventions that operate through image adaptation rather than access restriction. Future work should explore these approaches in more ecologically valid settings, over longer time scales, and with study designs better suited to isolating emotional mechanisms.

To support reproducibility, we plan to release the the source code of our algorithms and the experimental platform used in our studies upon acceptance.

## REFERENCES

- [1] Itzhak Aharon, Nancy Etcoff, Dan Ariely, Christopher F Chabris, Ethan O'connor, and Hans C Breiter. 2001. Beautiful faces have variable reward value: fMRI and behavioral evidence. *Neuron* 32, 3 (2001), 537–551.
- [2] Hosam Al-Samarraie, Kirfi-Aliyu Bello, Ahmed Ibrahim Alzahrani, Andrew Paul Smith, and Chikezie Emele. 2021. Young users' social media addiction: causes, consequences and preventions. *Information Technology & People* (2021). doi:10.1108/itp-11-2020-0753
- [3] Afsheen Rafaqat Ali and Mohsen Ali. 2017. Automatic image transformation for inducing affect. *arXiv preprint arXiv:1707.08148* (2017).
- [4] Jie An, Tianlang Chen, Songyang Zhang, and Jiebo Luo. 2021. Global Image Sentiment Transfer. In *2020 25th International Conference on Pattern Recognition (ICPR)*. IEEE, 6267–6274.
- [5] Cecilie Schou Andreassen. 2015. Online social network site addiction: A comprehensive review. *Current Addiction Reports* 2, 2 (2015), 175–184.
- [6] Apple. 2023. Keep track of your screen time on iPhone. [apple.com](https://apple.com) (Accessed: 11.01.2023).
- [7] Valeria Bekhtereva and Matthias M Müller. 2017. Bringing color to emotion: The influence of color on attentional bias to briefly presented emotional images. *Cognitive, Affective, & Behavioral Neuroscience* 17, 5 (2017), 1028–1047.
- [8] Jonah Berger and Katherine L Milkman. 2012. What makes online content viral? *Journal of marketing research* 49, 2 (2012), 192–205.
- [9] D.E. Berlyne. 1971. *Aesthetics and Psychobiology*. Appleton-Century-Crofts. <https://books.google.ch/books?id=o5TWWAAAAMAAJ>
- [10] Marco Bertamini, Alexis Makin, and Giulia Rampone. 2013. Implicit association of symmetry with positive valence, high arousal and simplicity. *i-Perception* 4, 5 (2013), 317–327.
- [11] Marco Bertamini, Giulia Rampone, Alexis DJ Makin, and Andrew Jessop. 2019. Symmetry preference in shapes, faces, flowers and landscapes. *PeerJ* 7 (2019), e7078.
- [12] Marco Bertamini, Juha Silvanto, Anthony M Norcia, Alexis DJ Makin, and Johan Wagemans. 2018. The neural basis of visual symmetry and its role in mid-and high-level visual processing. *Annals of the New York Academy of Sciences* 1426, 1 (2018), 111–126.
- [13] Lonni Besançon, Amir Semmo, David Biau, Bruno Frachet, Virginie Pineau, El Hadi Sariali, Rabah Taouachi, Tobias Isenberg, and Pierre Dragicevic. 2018. Reducing affective responses to surgical images through color manipulation and stylization. In *Expressive*. 11–1.

- [14] Anselm Brachmann and Christoph Redies. 2016. Using convolutional neural network filters to measure left-right mirror symmetry in images. *Symmetry* 8, 12 (2016), 144.
- [15] Anselm Brachmann and Christoph Redies. 2017. Computational and experimental approaches to visual aesthetics. *Frontiers in computational neuroscience* 11 (2017), 102.
- [16] Margaret M Bradley and Peter J Lang. 1994. Measuring emotion: the self-assessment manikin and the semantic differential. *Journal of behavior therapy and experimental psychiatry* 25, 1 (1994), 49–59.
- [17] William J. Brady, Julian A. Wills, John T. Jost, Joshua A. Tucker, and Jay J. Van Bavel. 2017. Emotion shapes the diffusion of moralized content in social networks. *Proceedings of the National Academy of Sciences* 114, 28 (2017), 7313–7318. doi:10.1073/pnas.1618923114
- [18] Sharon Brehm and Jack Brehm. 2013. *Psychological reactance: A theory of freedom and control*. Academic Press.
- [19] Tim Brooks, Aleksander Holynski, and Alexei A Efros. 2023. Instructpix2pix: Learning to follow image editing instructions. In *Proceedings of the IEEE/CVF Conference on Computer Vision and Pattern Recognition*. 18392–18402.
- [20] Moira Burke and Robert E. Kraut. 2016. The Relationship Between Facebook Use and Well-Being Depends on Communication Type and Tie Strength. *Journal of Computer-Mediated Communication* 21, 4 (05 2016), 265–281. arXiv:https://academic.oup.com/jcmc/article-pdf/21/4/265/22316334/jcmc0265.pdf doi:10.1111/jcc4.12162
- [21] Maya E Cano, Quetzal A Class, and John Polich. 2009. Affective valence, stimulus attributes, and P300: color vs. black/white and normal vs. scrambled images. *International Journal of Psychophysiology* 71, 1 (2009), 17–24.
- [22] Luis Carretié, Manuel Tapia, Sara López-Martín, and Jacobo Albert. 2019. EmoMadrid: An emotional pictures database for affect research. *Motivation and Emotion* 43 (2019), 929–939.
- [23] Junsong Chen, Shuchen Xue, Yuyang Zhao, Jincheng Yu, Sayak Paul, Junyu Chen, Han Cai, Song Han, and Enze Xie. 2025. Sana-sprint: One-step diffusion with continuous-time consistency distillation. *arXiv preprint arXiv:2503.09641* (2025).
- [24] Tianlang Chen, Wei Xiong, Haitian Zheng, and Jiebo Luo. 2020. Image sentiment transfer. In *Proceedings of the 28th ACM International Conference on Multimedia*. 4407–4415.
- [25] covenanteyes.com. 2022. CovenantEyes. [covenanteyes.com](https://covenanteyes.com) (Accessed: 08.07.2022).
- [26] Frederique Crete, Thierry Dolmiere, Patricia Ladret, and Marina Nicolas. 2007. The blur effect: perception and estimation with a new no-reference perceptual blur metric. In *Human vision and electronic imaging XII*, Vol. 6492. SPIE, 196–206.
- [27] Claudia Damiano, Dirk B Walther, and William A Cunningham. 2021. Cues to Danger: Contour Features Predict Valence and Threat Judgements in Scenes. (2021).
- [28] Elise S Dan-Glauser and Klaus R Scherer. 2011. The Geneva affective picture database (GAPED): a new 730-picture database focusing on valence and normative significance. *Behavior research methods* 43 (2011), 468–477.
- [29] Shengqi Dang, Yi He, Long Ling, Ziqing Qian, Nanxuan Zhao, and Nan Cao. 2025. Emoticrofter: Text-to-emotional-image generation based on valence-arousal model. In *Proceedings of the IEEE/CVF International Conference on Computer Vision*. 15218–15228.
- [30] DataReportal, & We Are Social, & Meltwater. 2023. Most popular websites worldwide as of November 2022, by total visits. <https://www.statista.com/statistics/1201880/most-visited-websites-worldwide/>
- [31] Andrea De Cesare and Maurizio Codispoti. 2010. Effects of picture size reduction and blurring on emotional engagement. *PLoS One* 5, 10 (2010), e13399.
- [32] Dian A. de Vries, A. Marthe Möller, Marieke S. Wieringa, Anniek W. Eigenraam, and Kirsten Hamelink. 2018. Social Comparison as the Thief of Joy: Emotional Consequences of Viewing Strangers' Instagram Posts. *Media Psychology* 21, 2 (April 2018), 222–245. doi:10.1080/15213269.2016.1267647
- [33] Sylvain Delplanque, Karim N'diaye, Klaus Scherer, and Didier Grandjean. 2007. Spatial frequencies or emotional effects?: A systematic measure of spatial frequencies for IAPS pictures by a discrete wavelet analysis. *Journal of neuroscience methods* 165, 1 (2007), 144–150.
- [34] Prafulla Dhariwal and Alexander Nichol. 2021. Diffusion models beat gans on image synthesis. *Advances in Neural Information Processing Systems* 34 (2021), 8780–8794.
- [35] forestapp.cc. 2018. Forest - Stay focused, be present. [forestapp.cc](https://forestapp.cc) (Accessed: 02.01.2023).
- [36] freedom.to. 2022. Freedom to be incredibly productive. [freedom.to](https://freedom.to) (Accessed: 08.07.2022).
- [37] Xiao-Ping Gao, John H Xin, Tetsuya Sato, Aran Hansuebsai, Marcello Scalzo, Kanji Kajiwara, Shing-Sheng Guan, Josep Valldeperas, Manuel José Lis, and Monica Billger. 2007. Analysis of cross-cultural color emotion. *Color Research & Application: Endorsed by Inter-Society Color Council, The Colour Group (Great Britain), Canadian Society for Color, Color Science Association of Japan, Dutch Society for the Study of Color, The Swedish Colour Centre Foundation, Colour Society of Australia, Centre Français de la Couleur* 32, 3 (2007), 223–229.
- [38] David Garcia, Arvid Kappas, Dennis Küster, and Frank Schweitzer. 2016. The dynamics of emotions in online interaction. *Royal Society open science* 3, 8 (2016), 160059.
- [39] Christoph Gebhardt and Robin Willardt. 2025. Effect of image adaptations on passive social media use (social media study). OSF Registrations, version v1. doi:10.17605/OSF.IO/QE3ZD
- [40] Christoph Gebhardt, Robin Willardt, and Christian Holz. 2024. Effect of image adaptations on passive social media use (refined). OSF Registrations, version v1. doi:10.17605/OSF.IO/52VYF
- [41] Gernot Gerger, Helmut Leder, Pablo PL Tinio, and Annkathrin Schacht. 2011. Faces versus patterns: Exploring aesthetic reactions using facial EMG. *Psychology of Aesthetics, Creativity, and the Arts* 5, 3 (2011), 241.
- [42] getcoldturkey.com. 2022. Cold Turkey - Your future self will thank you. [getcoldturkey.com](https://getcoldturkey.com) (Accessed: 08.07.2022).

- [43] Lore Goetschalckx, Alex Andonian, Aude Oliva, and Phillip Isola. 2019. Ganalyze: Toward visual definitions of cognitive image properties. In *Proceedings of the IEEE/CVF International Conference on Computer Vision*. 5744–5753.
- [44] Adam M Goodman, Jeffrey S Katz, and Michael N Dretsche. 2016. Military Affective Picture System (MAPS): A new emotion-based stimuli set for assessing emotional processing in military populations. *Journal of behavior therapy and experimental psychiatry* 50 (2016), 152–161.
- [45] Google. 2024. *Introducing Nano Banana Pro*. <https://blog.google/technology/ai/nano-banana-pro> Google Blog.
- [46] Natasha Gupta and Julia D. Irwin. 2016. In-class distractions: The role of Facebook and the primary learning task. *Computers in Human Behavior* 55 (2016), 1165–1178. doi:10.1016/j.chb.2014.10.022
- [47] Anke Haberkamp, Julia Anna Glombiewski, Philipp Schmidt, and Antonia Barke. 2017. The Disgust-Related-Images (DIRTI) database: Validation of a novel standardized set of disgust pictures. *Behaviour research and therapy* 89 (2017), 86–94.
- [48] Amanda C Hahn and David I Perrett. 2014. Neural and behavioral responses to attractiveness in adult and infant faces. *Neuroscience & Biobehavioral Reviews* 46 (2014), 591–603.
- [49] David Hasler and Sabine E Suesstrunk. 2003. Measuring colorfulness in natural images. In *Human vision and electronic imaging VIII*, Vol. 5007. SPIE, 87–95.
- [50] Jonathan Ho, Ajay Jain, and Pieter Abbeel. 2020. Denoising diffusion probabilistic models. *Advances in Neural Information Processing Systems* 33 (2020), 6840–6851.
- [51] Jonathan Ho and Tim Salimans. 2022. Classifier-free diffusion guidance. *arXiv preprint arXiv:2207.12598* (2022).
- [52] Jonathan Ho, Tim Salimans, Alexey Gritsenko, William Chan, Mohammad Norouzi, and David J Fleet. 2022. Video diffusion models. *Advances in neural information processing systems* 35 (2022), 8633–8646.
- [53] Yuanming Hu, Hao He, Chenxi Xu, Baoyuan Wang, and Stephen Lin. 2018. Exposure: A white-box photo post-processing framework. *ACM Transactions on Graphics (TOG)* 37, 2 (2018), 1–17.
- [54] Xun Huang, Ming-Yu Liu, Serge Belongie, and Jan Kautz. 2018. Multimodal unsupervised image-to-image translation. In *Proceedings of the European conference on computer vision (ECCV)*. 172–189.
- [55] Katherine Humphrey, Geoffrey Underwood, and Tony Lambert. 2012. Saliency of the lambs: A test of the saliency map hypothesis with pictures of emotive objects. *Journal of Vision* 12, 1 (2012), 22–22.
- [56] Aaron Hurst, Adam Lerer, Adam P Goucher, Adam Perelman, Aditya Ramesh, Aidan Clark, AJ Ostrow, Akila Welihinda, Alan Hayes, Alec Radford, et al. 2024. Gpt-4o system card. *arXiv preprint arXiv:2410.21276* (2024).
- [57] JDev. 2019. News Feed Eradicator. <chrome.google.com/nfe> (Accessed: 02.01.2023).
- [58] Jingyang Jia, Kai Shu, Gang Yang, Long Xing, Xun Chen, and Aiping Liu. 2025. EmoFeedback2: Reinforcement of Continuous Emotional Image Generation via LVLm-based Reward and Textual Feedback. *arXiv preprint arXiv:2511.19982* (2025).
- [59] Tero Karras, Miika Aittala, Tuomas Kynkäänniemi, Jaakko Lehtinen, Timo Aila, and Samuli Laine. 2024. Guiding a diffusion model with a bad version of itself. *Advances in Neural Information Processing Systems* 37 (2024), 52996–53021.
- [60] Hye-Rin Kim, Yeong-Seok Kim, Seon Joo Kim, and In-Kwon Lee. 2018. Building emotional machines: Recognizing image emotions through deep neural networks. *IEEE Transactions on Multimedia* 20, 11 (2018), 2980–2992.
- [61] Jaejeung Kim, Hayoung Jung, Minsam Ko, and Uichin Lee. 2019. GoalKeeper: exploring interaction lockout mechanisms for regulating smartphone use. *Proceedings of the ACM on Interactive, Mobile, Wearable and Ubiquitous Technologies* 3, 1 (2019), 1–29.
- [62] Seungbae Kim, Jyun-Yu Jiang, Masaki Nakada, Jinyoung Han, and Wei Wang. 2020. Multimodal Post Attentive Profiling for Influencer Marketing. In *Proceedings of The Web Conference 2020*. 2878–2884.
- [63] Minsam Ko, Subin Yang, Joonwon Lee, Christian Heizmann, Jinyoung Jeong, Uichin Lee, Daehee Shin, Koji Yatani, Junehwa Song, and Kyong-Mee Chung. 2015. NUGU: a group-based intervention app for improving self-regulation of limiting smartphone use. In *Proceedings of the 18th ACM conference on computer supported cooperative work & social computing*. 1235–1245.
- [64] Geza Kovacs, Zhengxuan Wu, and Michael S Bernstein. 2018. Rotating online behavior change interventions increases effectiveness but also increases attrition. *Proceedings of the ACM on HCI 2, CSCW* (2018).
- [65] Benedek Kurdi, Shayn Lozano, and Mahzarin R Banaji. 2017. Introducing the open affective standardized image set (OASIS). *Behavior research methods* 49 (2017), 457–470.
- [66] Peter J Lang, Margaret M Bradley, Bruce N Cuthbert, et al. 1997. International affective picture system (IAPS): Technical manual and affective ratings. *NIMH Center for the Study of Emotion and Attention* 1, 39-58 (1997), 3.
- [67] Christine Lavoie, Magali Dufour, Djamal Berbiche, Danyka Theriault, and Julie Lane. 2023. The relationship between problematic internet use and anxiety disorder symptoms in youth: specificity of the type of application and gender. *Computers in Human Behavior* 140 (2023), 107604.
- [68] Helmut Leder, Jussi Hakala, Veli-Tapani Peltoketo, Christian Valuch, and Matthew Pelowski. 2022. Swipes and Saves: A Taxonomy of Factors Influencing Aesthetic Assessments and Perceived Beauty of Mobile Phone Photographs. *Frontiers in Psychology* 13 (2022), 786977–786977.
- [69] Hsin-Ying Lee, Hung-Yu Tseng, Jia-Bin Huang, Maneesh Singh, and Ming-Hsuan Yang. 2018. Diverse image-to-image translation via disentangled representations. In *Proceedings of the European conference on computer vision (ECCV)*. 35–51.
- [70] Liu Yi Lin, Jaime E Sidani, Ariel Shensa, Ana Radovic, Elizabeth Miller, Jason B Colditz, Beth L Hoffman, Leila M Giles, and Brian A Primack. 2016. Association between social media use and depression among US young adults. *Depression and anxiety* 33, 4 (2016), 323–331.
- [71] Qing Lin, Jingfeng Zhang, Yew-Soon Ong, and Mengmi Zhang. 2025. Make me happier: Evoking emotions through image diffusion models. In *Proceedings of the IEEE/CVF International Conference on Computer Vision*. 16367–16376.

- [72] Tsung-Yi Lin, Michael Maire, Serge Belongie, James Hays, Pietro Perona, Deva Ramanan, Piotr Dollár, and C Lawrence Zitnick. 2014. Microsoft coco: Common objects in context. In *Computer Vision—ECCV 2014: 13th European Conference, Zurich, Switzerland, September 6–12, 2014, Proceedings, Part V 13*. Springer, 740–755.
- [73] Olatz Lopez-Fernandez, Lucia Romo, Laurence Kern, Amélie Rousseau, Bernadeta Lelonek-Kuleta, Joanna Chwaszcz, Niko Männikkö, Hans-Jürgen Rumpf, Anja Bischof, Orsolya Király, et al. 2023. Problematic internet use among adults: A cross-cultural study in 15 countries. *Journal of Clinical Medicine* 12, 3 (2023), 1027.
- [74] Danielle Lottridge, Eli Marschner, Ellen Wang, Maria Romanovsky, and Clifford Nass. 2012. Browser design impacts multitasking. In *Proceedings of the human factors and Ergonomics Society Annual Meeting*, Vol. 56. SAGE Publications Sage CA: Los Angeles, CA, 1957–1961.
- [75] Todd Love, Christian Laier, Matthias Brand, Linda Hatch, and Raju Hajela. 2015. Neuroscience of internet pornography addiction: A review and update. *Behavioral sciences* 5, 3 (2015), 388–433.
- [76] Cheng Lu, Yuhao Zhou, Fan Bao, Jianfei Chen, Chongxuan Li, and Jun Zhu. 2022. Dpm-solver++: Fast solver for guided sampling of diffusion probabilistic models. *arXiv preprint arXiv:2211.01095* (2022).
- [77] Tao Lu, Hongxiao Zheng, Tianying Zhang, Xuhai “Orson” Xu, and Anhong Guo. 2024. InteractOut: Leveraging Interaction Proxies as Input Manipulation Strategies for Reducing Smartphone Overuse. In *Proceedings of the CHI Conference on Human Factors in Computing Systems*. 1–19.
- [78] Kai Lukoff, Ulrik Lyngs, and Lize Alberts. 2022. Designing to support autonomy and reduce psychological reactance in digital self-control tools. In *Position Papers for the Workshop “Self-Determination Theory in HCI: Shaping a Research Agenda” at the Conference on Human Factors in Computing Systems (CHI’22)*, Vol. 5.
- [79] Ulrik Lyngs, Kai Lukoff, Laura Csuka, Petr Slovak, Max Van Kleek, and Nigel Shadbolt. 2022. The Goldilocks level of support: Using user reviews, ratings, and installation numbers to investigate digital self-control tools. *International journal of human-computer studies* 166 (2022), 102869.
- [80] Ulrik Lyngs, Kai Lukoff, Petr Slovak, Reuben Binns, Adam Slack, Michael Inzlicht, Max Van Kleek, and Nigel Shadbolt. 2019. Self-control in cyberspace: Applying dual systems theory to a review of digital self-control tools. In *proceedings of the 2019 CHI conference on human factors in computing systems*. 1–18.
- [81] Ulrik Lyngs, Kai Lukoff, Petr Slovak, William Seymour, Helena Webb, Marina Jirotko, Jun Zhao, Max Van Kleek, and Nigel Shadbolt. 2020. ‘I Just Want to Hack Myself to Not Get Distracted’: Evaluating Design Interventions for Self-Control on Facebook. In *Proceedings of the 2020 CHI Conference on Human Factors in Computing Systems (Honolulu, HI, USA) (CHI ’20)*. ACM, New York, NY, USA, 15 pages. doi:10.1145/3313831.3376672
- [82] Alexis DJ Makin, Moon M Wilton, Anna Pecchinenda, and Marco Bertamini. 2012. Symmetry perception and affective responses: A combined EEG/EMG study. *Neuropsychologia* 50, 14 (2012), 3250–3261.
- [83] Qi Mao, Haobo Hu, Yujie He, Difei Gao, Haokun Chen, and Libiao Jin. 2025. EmoAgent: Multi-Agent Collaboration of Plan, Edit, and Critic, for Affective Image Manipulation. *arXiv preprint arXiv:2503.11290* (2025).
- [84] Artur Marchewka, Łukasz Żurawski, Katarzyna Jednoróg, and Anna Grabowska. 2014. The Nencki Affective Picture System (NAPS): Introduction to a novel, standardized, wide-range, high-quality, realistic picture database. *Behavior research methods* 46 (2014), 596–610.
- [85] Maurizio Mauri, Pietro Cipresso, Anna Balgera, Marco Villamira, and Giuseppe Riva. 2011. Why Is Facebook So Successful? Psychophysiological Measures Describe a Core Flow State While Using Facebook. *Cyberpsychology, Behavior, and Social Networking* 14, 12 (Dec. 2011), 723–731. doi:10.1089/cyber.2010.0377
- [86] Youssef A Mejjati, Celso F Gomez, Kwang In Kim, Eli Shechtman, and Zoya Bylinskii. 2020. Look here! a parametric learning based approach to redirect visual attention. In *European Conference on Computer Vision*. Springer, 343–361.
- [87] Laura Miccoli, Rafael Delgado, Pedro Guerra, Francesco Versace, Sonia Rodríguez-Ruiz, and M Carmen Fernández-Santaella. 2016. Affective pictures and the Open Library of Affective Foods (OLAF): tools to investigate emotions toward food in adults. *PLoS one* 11, 8 (2016), e0158991.
- [88] Aswin Mohan. 2019. LessPhone. [play.google.com/apps/lessphone](https://play.google.com/apps/lessphone) (Accessed: 02.01.2023).
- [89] Ron Mokady, Amir Hertz, Kfir Aberman, Yael Pritch, and Daniel Cohen-Or. 2023. Null-text inversion for editing real images using guided diffusion models. In *Proceedings of the IEEE/CVF Conference on Computer Vision and Pattern Recognition*. 6038–6047.
- [90] Alberto Monge Roffarello and Luigi De Russis. 2019. The race towards digital wellbeing: Issues and opportunities. In *Proceedings of the 2019 CHI conference on human factors in computing systems*. 1–14.
- [91] David Mould, Regan L Mandryk, and Hua Li. 2012. Emotional response and visual attention to non-photorealistic images. *Computers & Graphics* 36, 6 (2012), 658–672.
- [92] Karen Nelson-Field, Erica Riebe, and Kellie Newstead. 2013. The Emotions that Drive Viral Video. *Australasian Marketing Journal* 21, 4 (2013), 205–211. doi:10.1016/j.ausmj.2013.07.003
- [93] Lauri Nummenmaa, Jari K Hietanen, Pekka Santtila, and Jukka Hyönä. 2012. Gender and visibility of sexual cues influence eye movements while viewing faces and bodies. *Archives of sexual behavior* 41, 6 (2012), 1439–1451.
- [94] Chanjong Park and In-Kwon Lee. 2020. Emotional landscape image generation using generative adversarial networks. In *Proceedings of the Asian Conference on Computer Vision*.
- [95] Eli Peli. 1990. Contrast in complex images. *JOSA A* 7, 10 (1990), 2032–2040.
- [96] Kuan-Chuan Peng, Tsuhan Chen, Amir Sadovnik, and Andrew C Gallagher. 2015. A mixed bag of emotions: Model, predict, and transfer emotion distributions. In *Proceedings of the IEEE conference on computer vision and pattern recognition*. 860–868.
- [97] Joanna Pilarczyk and Michał Kuniecki. 2014. Emotional content of an image attracts attention more than visually salient features in various signal-to-noise ratio conditions. *Journal of Vision* 14, 12 (2014), 4–4.

- [98] Charlie Pinder, Jose Ignacio Rocca, Benjamin R Cowan, and Russell Beale. 2019. Push away the smartphone: Investigating methods to counter problematic smartphone use. In *Extended Abstracts of the 2019 CHI Conference on Human Factors in Computing Systems*.
- [99] Dustin Podell, Zion English, Kyle Lacey, Andreas Blattmann, Tim Dockhorn, Jonas Müller, Joe Penna, and Robin Rombach. 2023. Sdxl: Improving latent diffusion models for high-resolution image synthesis. *arXiv preprint arXiv:2307.01952* (2023).
- [100] qustodio.com. 2022. Qustudio - parental control and digital wellbeing. [qustodio.com](https://qustodio.com) (Accessed: 08.07.2022).
- [101] Alec Radford, Jong Wook Kim, Chris Hallacy, Aditya Ramesh, Gabriel Goh, Sandhini Agarwal, Girish Sastry, Amanda Askell, Pamela Mishkin, Jack Clark, et al. 2021. Learning transferable visual models from natural language supervision. In *International conference on machine learning*. PMLR, 8748–8763.
- [102] Christoph Redies, Anselm Brachmann, and Johan Wagemans. 2017. High entropy of edge orientations characterizes visual artworks from diverse cultural backgrounds. *Vision Research* 133 (2017), 130–144.
- [103] Christoph Redies, Maria Grebenkina, Mahdi Mohseni, Ali Kaduhm, and Christian Dobel. 2020. Global image properties predict ratings of affective pictures. *Frontiers in psychology* 11 (2020), 953.
- [104] E. Riba, D. Mishkin, D. Ponsa, E. Rublee, and G. Bradski. 2020. Kornia: an Open Source Differentiable Computer Vision Library for PyTorch. In *Winter Conference on Applications of Computer Vision*. <https://arxiv.org/pdf/1910.02190.pdf>
- [105] Robin Rombach, Andreas Blattmann, Dominik Lorenz, Patrick Esser, and Björn Ommer. 2022. High-resolution image synthesis with latent diffusion models. In *Proceedings of the IEEE/CVF Conference on Computer Vision and Pattern Recognition*. 10684–10695.
- [106] James A. Russell. 1980. A circumplex model of affect. *Journal of Personality and Social Psychology* 39 (1980), 1161–1178. doi:10.1037/h0077714
- [107] Seyedmorteza Sadat, Otmar Hilliges, and Romann M Weber. 2024. Eliminating oversaturation and artifacts of high guidance scales in diffusion models. In *The Thirteenth International Conference on Learning Representations*.
- [108] Melanie Schreiner, Thomas Fischer, and Rene Riedl. 2021. Impact of content characteristics and emotion on behavioral engagement in social media: literature review and research agenda. *Electronic Commerce Research* 21 (2021), 329–345.
- [109] selfcontrolapp.com. [n. d.]. SelfControl. [selfcontrolapp.com](https://selfcontrolapp.com) (Accessed: 08.07.2022).
- [110] Jaana Simola, Kevin Le Fevre, Jari Torniaainen, and Thierry Baccino. 2015. Affective processing in natural scene viewing: Valence and arousal interactions in eye-fixation-related potentials. *NeuroImage* 106 (2015), 21–33.
- [111] Jiaming Song, Chenlin Meng, and Stefano Ermon. 2020. Denoising diffusion implicit models. *arXiv preprint arXiv:2010.02502* (2020).
- [112] Yuda Song, Zehao Sun, and Xuanwu Yin. 2024. Sdxs: Real-time one-step latent diffusion models with image conditions. *arXiv preprint arXiv:2403.16627* (2024).
- [113] Eva Specker, Helmut Leder, Raphael Rosenberg, Lisa Mira Hegelmaier, Hanna Brinkmann, Jan Mikuni, and Hideaki Kawabata. 2018. The universal and automatic association between brightness and positivity. *Acta Psychologica* 186 (2018), 47–53.
- [114] Shabbir Syed-Abdul, Luis Fernandez-Luque, Wen-Shan Jian, Yu-Chuan Li, Steven Crain, Min-Huei Hsu, Yao-Chin Wang, Dorjsuren Khandregzen, Enkhzaya Chuluunbaatar, Phung Anh Nguyen, and Der-Ming Liou. 2013. Misleading Health-Related Information Promoted Through Video-Based Social Media: Anorexia on YouTube. *Journal of Medical Internet Research* 15, 2 (Feb. 2013), e2237. doi:10.2196/jmir.2237
- [115] Vincent W-S Tseng, Matthew L Lee, Laurent Denoue, and Daniel Avrahami. 2019. Overcoming distractions during transitions from break to work using a conversational website-blocking system. In *Proc. of the 2019 CHI conference on human factors in computing systems*.
- [116] Oshin Vartanian, Vinod Goel, Elaine Lam, Maryanne Fisher, and Josipa Granic. 2013. Middle temporal gyrus encodes individual differences in perceived facial attractiveness. *Psychology of Aesthetics, Creativity, and the Arts* 7, 1 (2013), 38.
- [117] Soroush Vosoughi, Deb Roy, and Sinan Aral. 2018. The spread of true and false news online. *Science* 359, 6380 (2018), 1146–1151. doi:10.1126/science.aap9559
- [118] Tim Wu. 2017. *The attention merchants: The epic scramble to get inside our heads*. Vintage.
- [119] Yingjie Xia, Xi Wang, Jinglei Shi, Vicky Kalogeiton, and Jian Yang. 2025. MUSE: Manipulating Unified Framework for Synthesizing Emotions in Images via Test-Time Optimization. *arXiv preprint arXiv:2511.21051* (2025).
- [120] Heekyung Yang, Jongdae Han, and Kyungha Min. 2020. Emotion variation from controlling contrast of visual contents through EEG-Based deep emotion recognition. *Sensors* 20, 16 (2020), 4543.
- [121] Jingyuan Yang, Jiawei Feng, Weibin Luo, Dani Lischinski, Daniel Cohen-Or, and Hui Huang. 2025. Emoedit: Evoking emotions through image manipulation. In *Proceedings of the Computer Vision and Pattern Recognition Conference*. 24690–24699.
- [122] Kimberly Young. 2009. Understanding online gaming addiction and treatment issues for adolescents. *The American journal of family therapy* 37, 5 (2009), 355–372.
- [123] Jusheng Yu. 2014. We look for social, not promotion: Brand post strategy, consumer emotions, and engagement. *International Journal of Media & Communication* 1, 2 (2014), 28–37.
- [124] Sicheng Zhao, Chuang Lin, Pengfei Xu, Sendong Zhao, Yuchen Guo, Ravi Krishna, Guiguang Ding, and Kurt Keutzer. 2019. Cycleemotiongan: Emotional semantic consistency preserved cyclegan for adapting image emotions. In *Proceedings of the AAAI conference on artificial intelligence*, Vol. 33. 2620–2627.
- [125] Sicheng Zhao, Xin Zhao, Guiguang Ding, and Kurt Keutzer. 2018. Emotiongan: Unsupervised domain adaptation for learning discrete probability distributions of image emotions. In *Proceedings of the 26th ACM international conference on Multimedia*. 1319–1327.
- [126] Siqi Zhu, Chunmei Qing, Canqiang Chen, and Xiangmin Xu. 2022. Emotional Generative Adversarial Network for Image Emotion Transfer. *Expert Systems with Applications* (2022), 119485.

## A BACKGROUND: DIFFUSION MODELS

In this section, we adopt the notation of Mokady et al. [89] for clarity. For a detailed derivation of diffusion denoising probabilistic models, we refer readers to Ho et al. [50].

Text-guided diffusion models map a random noise vector  $z_t$  and a textual condition  $\mathcal{P}$  to an output image  $z_0$ , corresponding to the conditioning prompt. Sequential denoising is performed by training a network  $\epsilon_\theta$  to predict artificial noise, with the objective:

$$\min_{\theta} \mathbb{E}_{z_0, \epsilon \sim \mathcal{N}(0, I), t \sim \text{Uniform}(1, T)} \|\epsilon - \epsilon_\theta(z_t, t, C)\|^2. \quad (1)$$

$C = \psi(\mathcal{P})$  is the embedding of the text condition, and  $z_t$  is a noised version of the sampled data  $z_0$  at time step  $t$ . During inference, starting from a noise vector  $z_T$ , noise is progressively removed over  $T$  steps using the trained network.

As we intend to introduce subtle changes to a given real image, we employ deterministic DDIM sampling [111]:

$$z_{t-1} = \frac{\alpha_{t-1}}{\alpha_t} z_t + \left( \sqrt{\frac{1}{\alpha_{t-1}} - 1} - \sqrt{\frac{1}{\alpha_t}} \right) \cdot \epsilon_\theta(z_t, t, C). \quad (5)$$

For the definition of  $\alpha_t$  see Section A.1.

Diffusion models can operate in image pixel space, with  $z_0$  representing a real image sample. In our work, we utilize the SDXL model [99], where the forward diffusion process is applied to a latent image encoding  $z_0 = E(I)$ , and an image decoder is used at the end of the reverse diffusion process to produce  $I = D(z_0)$ .

### A.1 Forward diffusion process

The forward diffusion process is presented here for completeness and can be defined as follows:

$$z_t = \sqrt{\alpha_t} z_0 + \sqrt{1 - \alpha_t} \cdot \epsilon, \quad \epsilon \sim \mathcal{N}(0, I), \quad (6)$$

where  $\alpha_t = \prod_{i=1}^t (1 - \beta_i)$  is the cumulative product of the noise schedule and  $\beta = \{\beta_1, \beta_2, \dots, \beta_T\}$  is the noise schedule controlling the diffusion process.  $\epsilon \sim \mathcal{N}(0, I)$  represents Gaussian noise sampled at each step.

### A.2 Classifier guidance

To improve control and precision during the denoising process, classifier guidance was proposed as a post-hoc conditioning mechanism for diffusion models [34]. This method modifies the noise prediction process by incorporating a gradient term derived from a classifier  $p_\phi(y|z_t)$ , where  $y$  denotes the conditioning input:

$$\hat{\epsilon}_\theta(z_t, t, C, y) = \epsilon_\theta(z_t, t, C) + s \cdot \nabla_{z_t} \log p_\phi(y|z_t). \quad (7)$$

Here,  $\epsilon_\theta(z_t, t)$  is the original noise prediction,  $s$  is a guidance scale parameter that controls the strength of the classifier’s influence, and  $\nabla_{z_t} \log p_\phi(y|z_t)$  denotes the gradient of the log-probability of  $y$  with respect to  $z_t$ . By incorporating the classifier’s gradient, the denoising process is guided towards samples that better match the desired conditioning  $y$ .

### A.3 Classifier-free guidance

Another approach that offers posthoc conditional control over the denoising process is classifier-free guidance (CFG) [51]. It enhances the effect of conditioned text by combining an additional unconditional prediction with the conditioned prediction through extrapolation. Formally, let  $\emptyset = \psi(\text{""})$  represent the embedding of a null text, and let  $w$  denote the

guidance scale parameter. The classifier-free guidance prediction is given by:

$$\hat{\epsilon}_\theta(z_t, t, C, \theta) = w \cdot \epsilon_\theta(z_t, t, C) + (1 - w) \cdot \epsilon_\theta(z_t, t, \theta). \quad (8)$$

#### A.4 DDIM inversion

DDIM inversion [34, 111] offers a straightforward approach to reverse DDIM sampling based on the assumption that the ODE process can be reversed with sufficiently small steps. The inversion process is described by:

$$z_{t+1} = \frac{\alpha_{t+1}}{\alpha_t} z_t + \left( \sqrt{\frac{1}{\alpha_{t+1}} - 1} - \sqrt{\frac{1}{\alpha_t}} \right) \cdot \epsilon_\theta(z_t, t, C). \quad (9)$$

Essentially, the diffusion process is reversed, transitioning from  $z_0 \rightarrow z_T$  rather than the forward process of  $z_T \rightarrow z_0$ , where  $z_0$  represents the encoding of the given real image.

#### A.5 Null-text optimization

NTO [89] addresses the issue of DDIM inversion with CFG leading to visual artifacts and reduced editability of the inverted noise vector. It initializes  $\tilde{z}_T = z_T^*$  using the sequence of noisy latent codes  $z_T^*, \dots, z_0^*$  produced by DDIM inversion, where  $z_0^* = z_0$ . Then, it optimizes the timestamps  $t = T, \dots, 1$  with a fixed guidance scale  $w$  by minimizing:

$$\min_{\theta_t} \left\| z_{t-1}^* - z_{t-1}(\tilde{z}_t, \theta_t, C) \right\|^2. \quad (3)$$

Here,  $z_{t-1}(\tilde{z}_t, \theta_t, C)$  denotes a DDIM sampling step using  $\tilde{z}_t$ , the unconditional embedding  $\theta_t$ , and the conditional embedding  $C$ . At each step,  $\tilde{z}_{t-1}$  is updated as  $\tilde{z}_{t-1} = z_{t-1}(\tilde{z}_t, \theta_t, C)$ . With the optimized noise  $\tilde{z}_T = z_T^*$  and unconditional embeddings  $\{\theta_t\}_{t=1}^T$ , the input image can be de-noised while retaining editability.

## B DATASET

The integrated dataset shows the strong correlation between high and low valence with high arousal, commonly found in emotional ratings (see Figure 13).

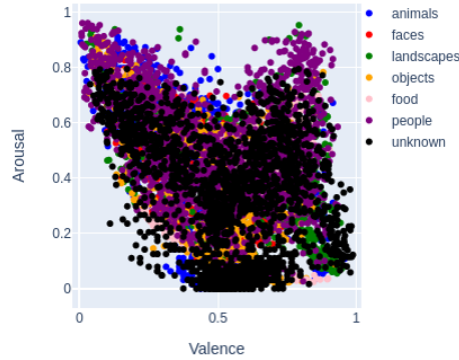


Fig. 13. Location of stimuli of our integrated dataset within the valence arousal space of the Circumplex Model of Affect [106].

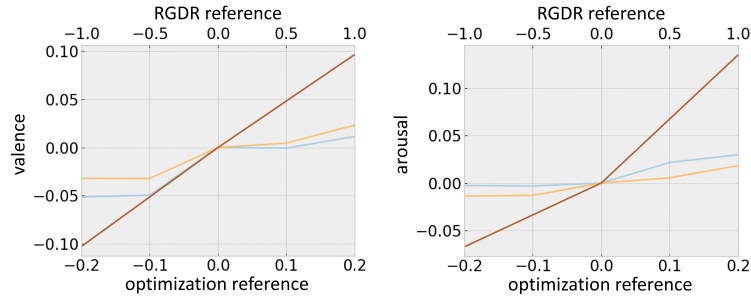


Fig. 14. Bidirectional emotional changes: The plots show how predicted valence and arousal evolve as the emotional reference of style optimization, parametric optimization, and RGDR is changed. In each plot, the lower x-axis represents the emotional reference for parametric optimization and style optimization, while the upper x-axis indicates the emotional reference for RGDR. The values at 0.0 represent the original image’s valence and arousal.

## C BIDIRECTIONAL EMOTIONAL CHANGES

To further assess the effectiveness of approaches, we run an experiment to determine whether RGDR, style optimization, and parametric optimization can optimize images for different reference points in the valence-arousal space.

For style optimization and parametric optimization, which primarily modify color values, initial experiments revealed that extreme emotional references often introduce artifacts (e.g., images becoming entirely black). Therefore, we define their reference points relative to the inferred valence and arousal values of each image. Specifically, we selected incremental adjustments of  $[-0.2, -0.1, +0.1, +0.2]$  to both valence and arousal values as targets for optimization, with values clipped to the interval  $[0, 1]$ . In contrast, RGDR was able to accommodate more extreme emotional references. We therefore used larger adjustments of  $[-1.0, +1.0]$  for both valence and arousal, again constraining results to  $[0, 1]$ .

This experiment is conducted on a random subset of 500 images from the Instagram Influencer Dataset [62]. We use the same weights for the approaches as in the image rating study (RGDR:  $w = 2.0, s = 0.2$ ; style optimization:  $w_1 = 1.0, w_2 = 0.2$ ; and parametric optimization:  $w_1 = 1.0, w_2 = 0.2$ ).

### C.1 Results

Figure 14 illustrates the emotional reference values plotted against the averaged inferred valence and arousal of all adapted images. The results indicate that the adaptation approaches achieve the intended directional emotional changes, albeit to a lesser degree than the reference values. RGDR demonstrates a steeper positive slope for both valence and arousal compared to style optimization and parametric optimization.

Qualitative inspection of the results reveals distinct trends across the approaches. For style optimization and parametric optimization, an increase in the valence and arousal reference results in warmer colors in the adapted images, while more negative values typically yield cooler tones (subfigures b and c in Figures 15 & 16, and 17). In contrast, RGDR introduces plastic changes, such as making subjects appear more attractive and enhancing their smiles as the emotional reference increases (Figures 15 and 17). Additionally, RGDR produces images with greater detail and saturation as the emotional reference intensifies (Figure 16).

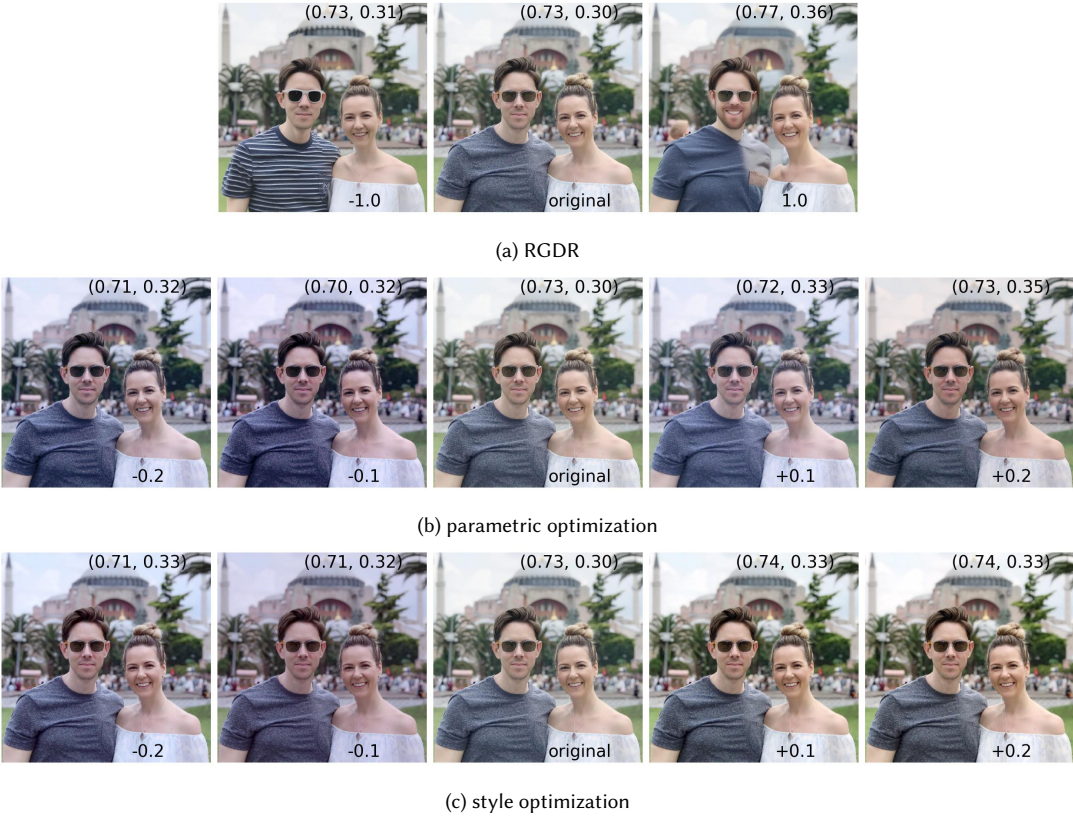


Fig. 15. Example result of bidirectional emotional change analysis. The emotional reference is displayed in the bottom-right corner, while the inferred valence and arousal values are shown in the top-right corner [format: (valence, arousal)]. Image caption: "A man and a woman standing closely with a historical building in the background."

**C.2 Discussion**

All approaches produced meaningful changes in response to different emotional references, with RGDR exhibiting stronger directional effects than style optimization and parametric optimization. The weaker correspondence between reference values and outcomes is attributable to the dual-objective optimization, which balances emotional modulation against fidelity to the original images. Qualitative inspection reveals distinct trends: style optimization and parametric optimization use warmer tones for higher valence/arousal and cooler tones for lower values. RGDR introduces plastic changes, such as enhancing smiles and perceived attractiveness as valence and arousal increase.

**D ADDITIONAL QUALITATIVE RESULTS FROM THE CRITERIA ALIGNMENT EXPERIMENT**

Figures 18, 19, and 20 show further qualitative results of the criteria alignment experiment.

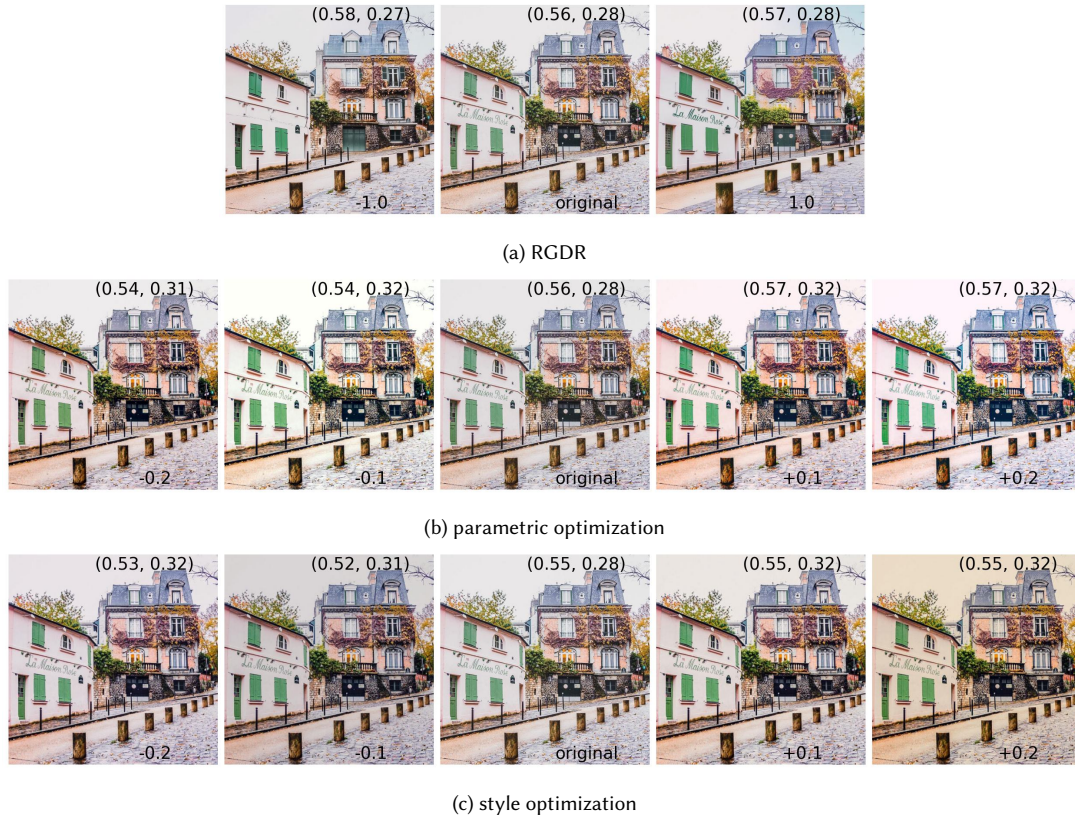


Fig. 16. Example result of bidirectional emotional change analysis. The emotional reference is displayed in the bottom-right corner, while the inferred valence and arousal values are shown in the top-right corner [format: (valence, arousal)]. Image caption: "A serene, narrow street with cobblestones, a pink house with green shutters, and a multi-story building with ivy."

## E SUPPLEMENTARY INFORMATION FOR SOCIAL MEDIA STUDY

### E.1 Feed

Figure 21 depicts the social media feed of our experimental platform, as used in the social media study.

### E.2 Adapted social media images

Figure 22 shows further examples of adapted images used in the social media study.

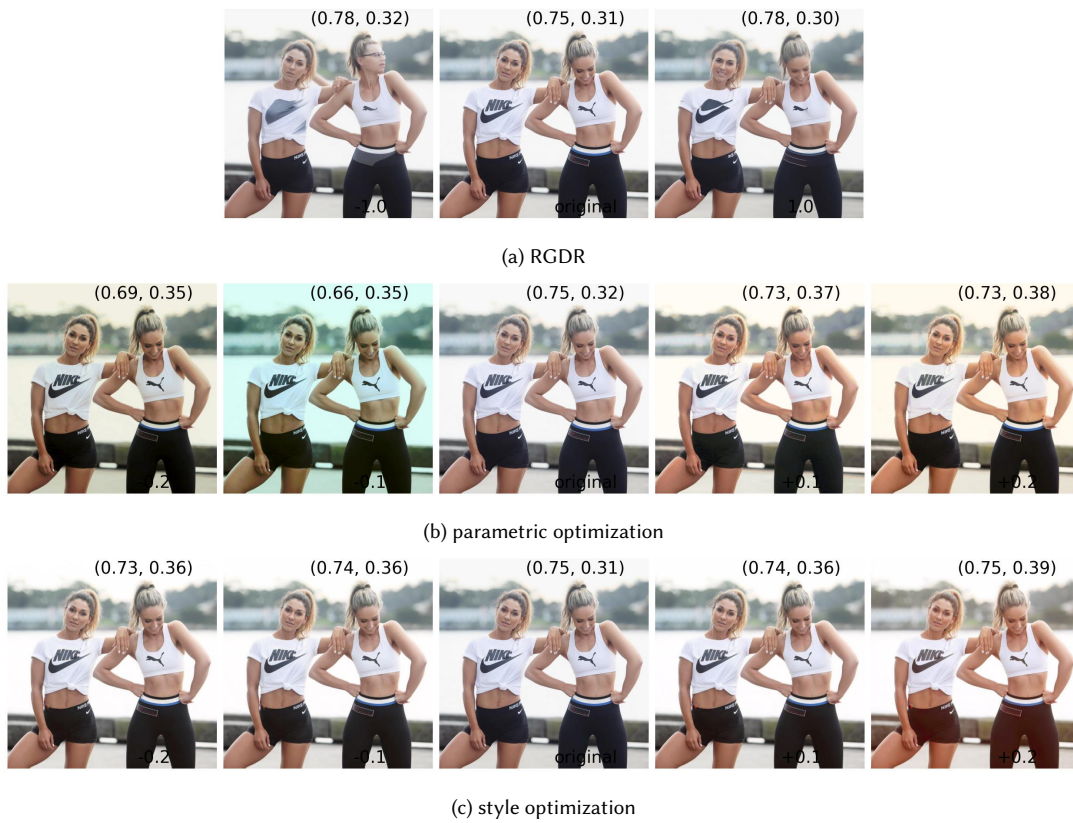


Fig. 17. Example result of bidirectional emotional change analysis. The emotional reference is displayed in the bottom-right corner, while the inferred valence and arousal values are shown in the top-right corner [format: (valence, arousal)]. Image caption: "Two women in athletic wear posing outdoors near a body of water."

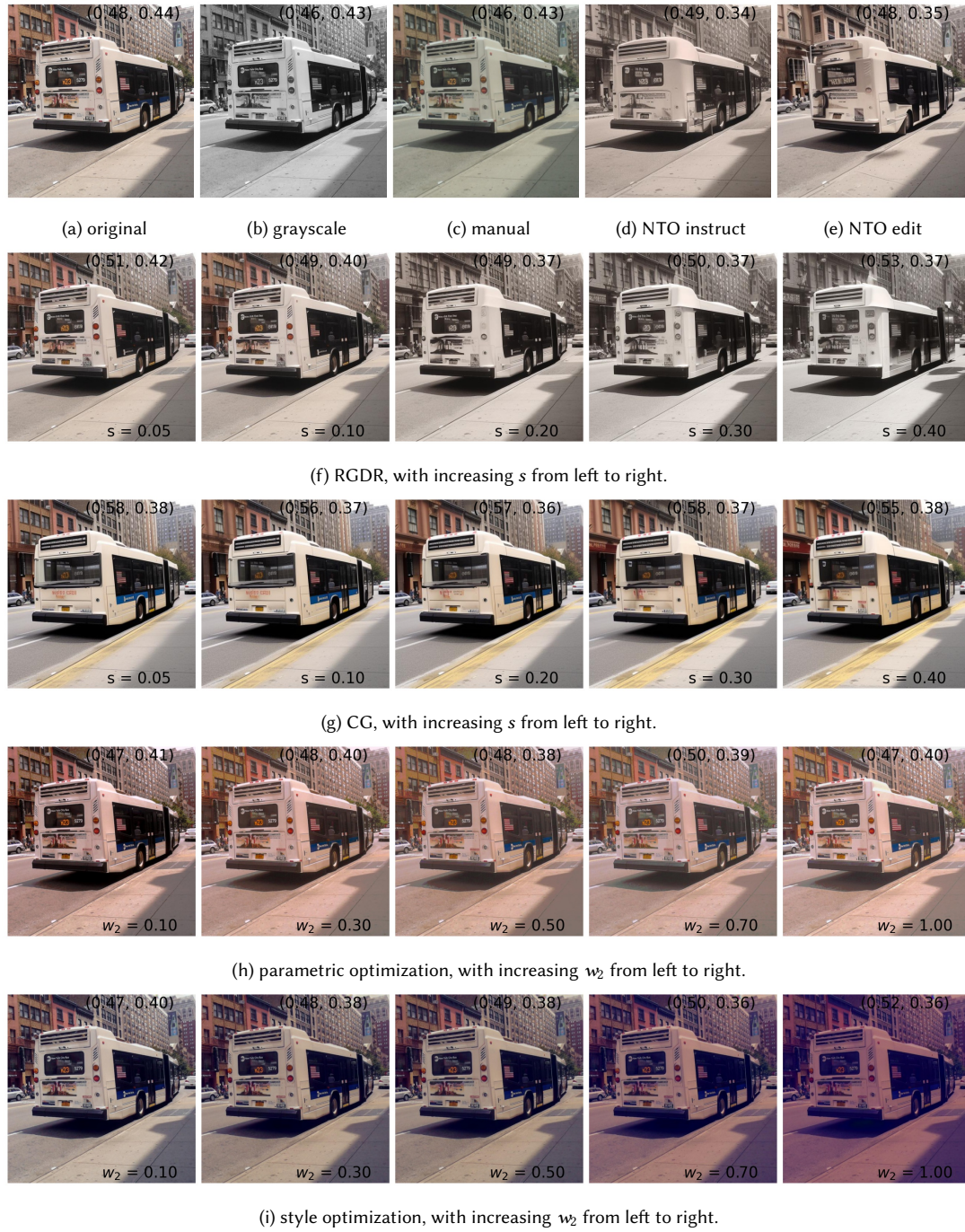


Fig. 18. Example result. Predicted valence–arousal values are shown top-right [target: (valence = 0.5, arousal = 0.0)].



Fig. 19. Example result. Predicted valence-arousal values are shown top-right [target: (valence = 0.5, arousal = 0.0)].

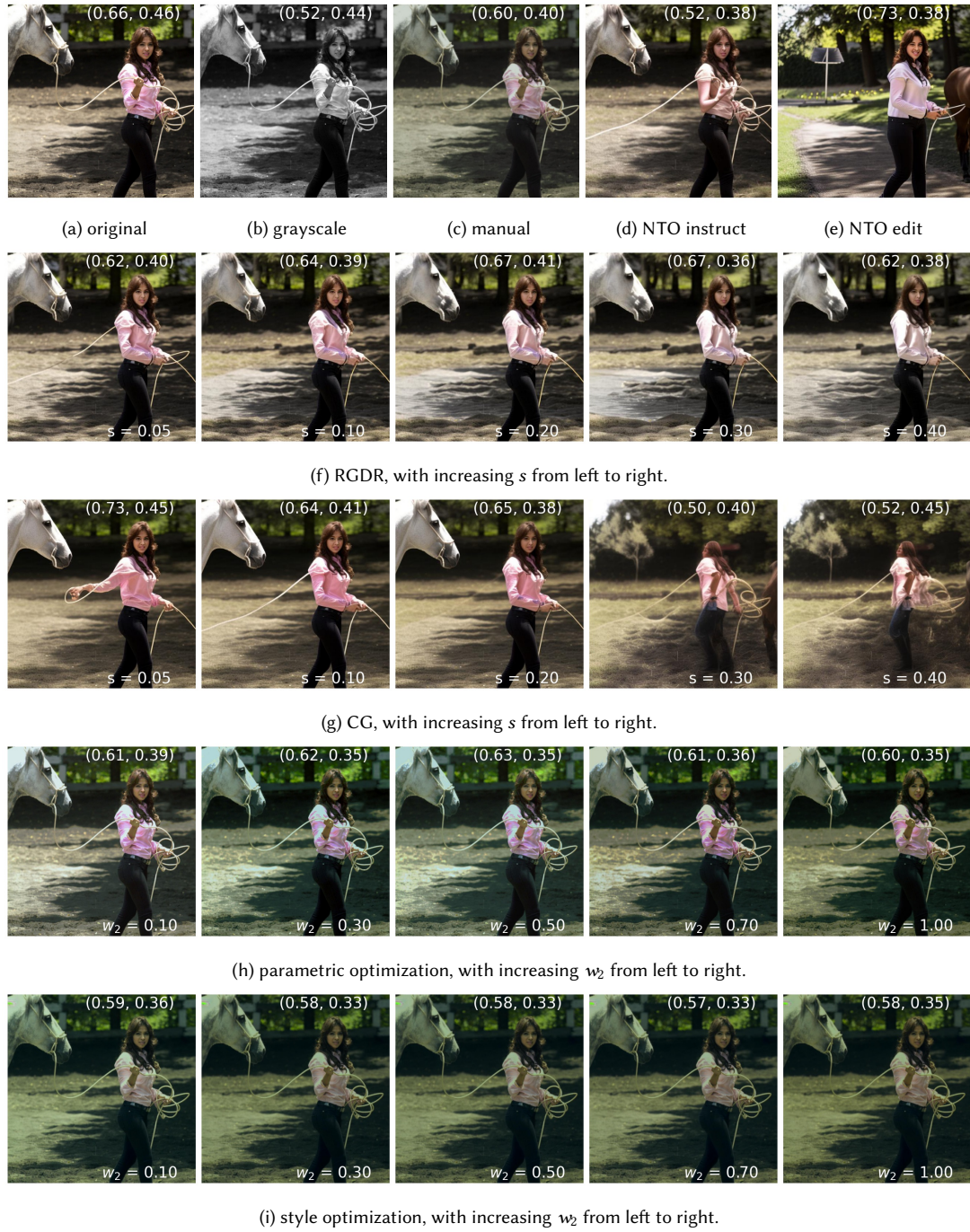


Fig. 20. Example result. Predicted valence–arousal values are shown top-right [target: (valence = 0.5, arousal = 0.0)].



2198 likes

**andrewkuttler** A flower for @asenseofhuber 🌸

23 comments

**technopaul**  
Moraine Lake



2167 likes

**technopaul** "Be anxious for nothing. You're safe. You can rest." - @maxlucado // praying for Texas today and the... more

115 comments

**globetrotter\_kt**  
Horseshoe Bend



Fig. 21. Illustration of social media feed on our platform.



(a) Subjects get older. Caption: "A woman in athletic wear sits on a bed holding a mug with a packet of FITWHEY protein powder beside her."



(b) Subjects decline in attractiveness. Caption: "Two individuals standing close to each other in a room with framed artwork."



(c) Subjects get clothed. Caption: "Woman in striped bikini stands in front of a modern white building with balconies."



(d) Subjects' facial expression is changed. Caption: "'Bride and groom in traditional attire in front of a fountain'."



(e) Subjects get removed. Caption: "Hand holding a yellow flower with a person standing in a field behind."



(f) Subjects are reduced in size. Caption: "A dog standing on a rocky ledge above a small waterfall in a forest."



(g) Animals appear less cute. Caption: "A woman running on the beach with a dog on a leash."



(h) Background becomes simpler. Caption: "A person jumps joyfully among string lights at night in a garden."

Fig. 22. Social media images adapted with RGDR, each illustrating a typical change it induces (see sub-caption).